Division of Pharmaceutical Chemistry and Technology
Faculty of Pharmacy
University of Helsinki
Finland

Evaluating mechanical properties and tabletability of pharmaceutical powders with a novel gravitation-based high-velocity compaction method

by

Timo Tanner

DOCTORAL DISSERTATION

To be presented for public discussion with the permission of the Faculty of Pharmacy of the University of Helsinki in room 2402, Biocenter 3 (Viikinkaari 1, Helsinki), on the 29th of March, 2021 at 17 o'clock.

Helsinki 2021

Supervisors

Professor Jouko Yliruusi (Emeritus)
Division of Pharmaceutical Chemistry and Technology
Faculty of Pharmacy
University of Helsinki
Finland

Professor Anne Juppo
Division of Pharmaceutical Chemistry and Technology
Faculty of Pharmacy
University of Helsinki
Finland

Doctor Osmo Antikainen
Division of Pharmaceutical Chemistry and Technology
Faculty of Pharmacy
University of Helsinki
Finland

Doctor Henrik Ehlers
Division of Pharmaceutical Chemistry and Technology
Faculty of Pharmacy
University of Helsinki
Finland

Reviewers

Professor Jarkko Ketolainen
School of Pharmacy
Faculty of Health Sciences
University of Eastern Finland

Professor João Pinto
Department of Galenic Pharmacy
and Pharmaceutical Technology
Faculty of Pharmacy
University of Lisbon

Opponent

Professor Changquan Calvin Sun
Department of Pharmaceutics
College of Pharmacy
University of Minnesota

ISBN 978-951-51-7147-4 (pbk.)
ISBN 978-951-51-7148-1 (PDF)

Unigrafia
Helsinki 2021

Abstract

Developing new pharmaceuticals is costly and time-consuming. New methods are always in demand for various stages of product development. Investing in the early phases of development can save a significant amount of resources in the long term.

Tablet is still the most commonly used pharmaceutical dosage form. Tablets are often produced by powder compression. Powder particles fragment and deform under pressure, allowing new bonds to form between them. Modern machines can produce over one million tablets per hour.

The mechanical properties of the powders have a remarkable impact on compact formation. For example, excessive elasticity in a powder mixture can lead to weak or defected tablets being produced. Therefore, the mechanical properties need to be studied. Devices known as tableting simulators have been designed to aid in developing adequate tablet formulations. These machines are useful, but they can still be quite expensive and large. The results obtained by these machines are not always universally applicable, and further interpretation is often required.

In this thesis, a novel gravitation-based high-velocity compaction (G-HVC) method was developed to study the compressibility and tabletability of powders in a cost-efficient and straightforward manner. The method is based on a freely falling steel bar, which compresses the powder sample inside a custom-made die. The movement of the bar and the deformation wave of the system base were monitored by high-accuracy displacement sensors. Displacement graphs could then be derived further. All data obtained by the method was ultimately only based on the displacement data.

First, microcrystalline cellulose (MCC) and starch samples were compressed to demonstrate the functionality of the method. MCC was shown to be more compressible and less elastic than starch. Apparent differences in the relative volume decrease and the compression behaviour of these two materials could be seen.

Next, various materials were studied more comprehensively. Two different setups with varying pressure were in use. Lactose grades and glucose showed effective fragmentation and reached true density with both setups. MCC grades were clearly pressure-dependent and showed slower gradual deformation, indicating plastic behaviour. Compression pressure was not high enough to effectively fragment calcium phosphate. Starch showed most elasticity of all the samples. In summary, all examined materials could be successfully categorized in terms of their mechanical properties.

Finally, the practical relevance of the method was shown by creating a model between the compaction energy values determined by G-HVC method and the tensile strength of tablets produced with a tableting machine. Three different formulations consisting of MCC, calcium phosphate, theophylline and HPMC were granulated utilizing a fluid bed system. There was a good correlation between compaction energy and tensile strength.

In summary, the G-HVC method was proven to be a reliable and cost-efficient tool in the examination of the mechanical properties of powders. The method was also capable of producing practically relevant results. The method fits well in modern pharmaceutical research where material-sparing, straightforward and reliable methods are in demand.

Acknowledgements

March 22nd, 2020, Helsinki. Spring is on its way. During the last month, I've mostly stayed indoors, staring at my laptop screen and writing this book. The world is going through a calamity right now, and most of the people are spending time in quarantine, more or less. Guess I got a bit lucky as I would have worked from home in any case. This adversity, too, will pass and the new seasons will come.

The schedule was tight, but the work for the PhD degree is now done for the most part. *Fly High Fall Far* by *Pendragon* can be heard on my headset, one of the songs that have given me energy to keep going. My new *Roland* keytar has mostly spent its days in the corner of my room, unfortunately. I wish I'll have more time for music in the near future as I think I'm going slightly mad without it. I just realized I haven't seen my bandmates in a year or so! Balancing between work and studies, the last 12 months have been tough, there is no doubt about it. However, the future ahead looks nice and hazy, opportunities here and there. Yet not a clue where I'm going to end up. Just the way I like it.

Let's go back in time a little bit. I had scheduled a meeting with Jouko Yliruusi to discuss my Master's Thesis. It was the end of the year 2015, something like that. Jouko told me that they have created a new invention with Osmo Antikainen. Some sort of a tableting machine that makes a lot of noise. My classmate, Jasmina Ikonen, had written her Master's about the first prototype. I feel you, Jasmina, it must have been a ton of work. And for that work I'm very grateful. Your work was a stepping stone for the studies ahead.

The new model was a huge improvement over the previous one. The device eventually had a plethora of names, some called it *GraviComp* and some called it *G-Press*. Gee, I wonder what this machine does? In the end, the method itself was more important than the device and we settled with the G-HVC method. The names don't matter because here's the important part: Jouko and Osmo asked me to basically "go crazy" with the device. "Do whatever, see what you can get out of it", basically. I had always wanted a job that required creativity and for the first time ever, I was there. Henrik Ehlers and Heikki Räikkönen also joined the team and with everyone's contribution we started discovering all the possibilities there was to find. Some years later, three articles and a book exist. Not bad for an idea that is rumoured to have been given birth in a sauna.

Jouko, I am eternally grateful that you took me in and believed in me. I needed that trust. Thank you, Osmo, Henrik and Heikki, for all the hard work and teaching you have done over the years. We rarely had a bad day, and I'll always cherish our passionate discussions. Also, a huge thank you to Anne Juppo, who inherited Jouko's students after his retirement. Even though our collaboration was quite short, we were an effective team. Thank you, David Blanco and Arne Pollet, for "spending time in the cell" with me during some of the experiments. Your contribution was imperative for the quality of the articles too. Also, thank you Jyrki Heinämäki and Juha Kiesvaara for serving as my follow-up group, monitoring my progress. And also, special thanks to Tuomas Saarinen for professional and mental support. In general, a huge thank you to all my colleagues in Division of Pharmaceutical Chemistry and Technology. I'd also like to acknowledge The Finnish Cultural Foundation and the University of Helsinki for financial support.

I could thank Doctor Jukka Saarinen and Doctor Sami Svanbäck for many reasons. Let's start with the professional side. You do know that I basically copied everything from your Theses which are sitting valiantly on my shelf? Well, not the contents, of course, but I did double-check many technical aspects. I placed your books next to me every time I wrote, so thank you for showing me the way. Next, thank you for recruiting me to Doctor Doctor, possibly the most kind-hearted rock band in the world. It has been my fortune that organ players are rare to come by. Playing both in practice and live with you guys has been amazing. Also, thank you, Frank, for lighting up the crowd with your voice, and well, lighting us all on fire during practice. Thank you, Tuukka, our drummer, for the melodies. Thank you, Andy, our most recent bassist for sticking with us and having a good time with us. Also, thanks to all the previous bassists, you know who you are. I hope we can practice again soon and start polishing those original tracks. I'll try and not steal the show with my flashy new keytar!

Thank you, Olli and Markus, for both friendship and the music. Olli, first we were classmates in elementary school and now we'll most likely graduate as doctors the same year too. I wish the best of health to you. And remember, I have my *Ren & Stimpy* DVD ready any time. Markus, call the police…

Thank you, Jaakko, Tero, Ville and Pekka for the friendship and for the party. No one would believe some of the adventures we've gone through. Boy, do we have to remain tight-lipped in each other's weddings… Pekka, we have known since Hämeenlinna times, and I'll always cherish our time together. Remember that you are an amazing musician and that the world needs to hear your creativity. Best of health to you and your family. Also, thank you, Jasmin and Aino for your friendship and the partying. Iina, thank you for the friendship and for being the best friend to the-one-whom-shall-be-named-a-bit-later.

I'd like to definitely thank my amazing colleagues from Hämeenlinnan Tori-Apteekki. We have known for over ten years, and you guys have always known how to have a good time! My fate takes me elsewhere, but I will never forget the times we've had. Also, special thanks to Marketta and Jukka for giving me shifts. You do know that a remarkable portion of this work was funded by the salary I received from you?

Next, I'd like to thank my mother Paula, my father Reijo, brethren Ville and Kimmo, and my sister Maria for all the support over the years. We only have the time to see each other a couple of times each year, which is hard at times. But I know that you all believed in me and that is more than enough. Also, thank you, Marjo and Ahti. I'd like to present special thanks to my mother, who has always pushed me forward in my studies. You saw my potential for this degree ever since I was a little kid. I guess you were right.

Last, but definitely not least, a person who entered my life on a fateful evening, in a place, where I didn't expect to find her. Satu, meeting you has changed me, and made me a better person. I'm not gonna go with any old cliché, that I wouldn't have gotten the degree without you or any of that poppycock. I do have an angle, though. The old me would have anxiously banged his head on the wall until this work was done, and failure could have crushed me. But now that I've met you, I feel like taking another path wouldn't have been too bad, as long as I could've taken that path with you. Let's stay gold.

I’m terribly sorry if I forgot to mention anyone, but you know who you are. And with that, peace of mind, happiness and good health to everyone!

Timo Juho Wiljam Tanner

Everyone is a genius.
But if you judge a fish by its ability to climb a tree,
it will live its whole life believing that it is stupid.

-Anonymous-

Fly high, fall far
Keep your fingers crossed, keep your ears to the floor
When the ferryman comes to take his fee
What you once owned is no longer yours
But love is free

-Nick Barrett, Pendragon-

In a world where I feel so small
I can't stop thinking big

-Neil Peart, Rush

This one goes out to the ones I love

Table of contents

List of original publications

This thesis is based on the following publications:

I **Tanner, T.**, Antikainen O., Ehlers H., Yliruusi, J., Introducing a novel gravitation-based high-velocity compaction analysis method for pharmaceutical powders. International Journal of Pharmaceutics, 526: 31–40, 2017.

II **Tanner T.**, Antikainen O., Ehlers H., Blanco D., Yliruusi J., Examining mechanical properties of various pharmaceutical excipients with the gravitation-based high-velocity compaction analysis method. International Journal of Pharmaceutics, 539: 131–138, 2018.

III **Tanner T.**, Antikainen O., Pollet A., Räikkönen H., Ehlers H., Juppo A., Yliruusi J., Predicting tablet tensile strength with a model derived from the gravitation-based high-velocity compaction analysis data. International Journal of Pharmaceutics, 566: 194–202, 2019.

The publications are referred to in the text by their roman numerals.

Abbreviations

A	Constant in Heckel's plot
ADMET	Absorption, distribution, metabolism, excretion and toxicity
API	Active pharmaceutical ingredient
AUC	Area under the curve
G-HVC	Gravitation-based high-velocity compaction
d	Diameter
D	Density
D_a	Apparent density
DCP	Dicalcium phosphate dihydrate
D_r	Relative density
D_t	True density
E	Internal energy
E_{comp}	Compaction energy
E_{comp5}	Compaction energy during the fifth compression
el_{iia}	Immediate in-die axial elastic recovery
E_{ml}	Machine-originated energy loss
E_{ml5}	Machine-originated energy loss during the fifth compression
E_{ne}	Total non-elastic energy
E_{ne5}	Total non-elastic energy during the fifth compression
E_{rec}	Energy consumed in immediate elastic recovery
E_{rec5}	Elastic energy during the fifth compression
E_{sl}	Sample-originated energy loss
E_{tot}	Total input energy
E_y	Young's modulus
ER	Elastic recovery
F	Force
FBG	Fluid bed granules
F_c	Crushing strength
F_0	Force at time zero
g	Gravitational acceleration
GI	Gastrointestinal
H	Tablet height
h_a	The powder bed height after the compression
h_c	Lowest powder bed height during the compression
HPMC	Hydroxypropyl methylcellulose
HRC	Hardness Rockwell C scale
k	Coefficient in Maxwell's model
K	Coefficient in Heckel's plot
kHz	Kilohertz
kg	Kilogram
K_{Ic}	Critical stress intensity factor
ln	Natural logarithm

m	Metre
M	Mass (measured as weight)
MCC	Microcrystalline cellulose
mg	Milligram
mm	Millimetre
ms	Millisecond
MPa	Megapascal
NME	New molecular entity
P	Pressure
P_d	Deformation hardness
P_f	Fracture pressure
PM	Physical mixture
P_{max}	Theoretical maximum deformation hardness
P_y	Mean yield pressure
P_{yh}	Yield pressure at the highest compression speed
P_{yl}	Yield pressure at the lowest compression speed
Ph. Eur.	European Pharmacopoeia
PD	Pharmacodynamics
PK	Pharmacokinetics
QbD	Quality by design
R	Fracture toughness
R&D	Research & development
R^2	Coefficient of determination
s	Second
SRS	Strain rate sensitivity
t	Time
USD	United States dollar
USP	United States Pharmacopeia
V_{bmax}	Maximum base velocity
vs	Versus
w/w	Weight percentage
w_s	Sample mass (measured as weight)
y_{final}	Final displacement level
y_{init}	Initial falling height
y_{mach}	Machine deformation
y_{max}	Detected maximum displacement
y_{maxt}	True maximum displacement
y_{reb}	The highest rebound height
γ	Compression susceptibility
ε	Strain
µm	Micrometre
µs	Microsecond
ν	Poisson's ratio
σ_t	Tensile strength

1 Introduction

The research and development (R&D) of new molecular entities (NME) consumes both time and money. Development of NME can take 10-15 years on rough average and cost nearly 3 billion USD (Paul et al. 2010, DiMasi et al. 2016). While the annual number of approved NMEs has stayed roughly the same since the 1950s, the R&D costs have increased remarkably (Munos 2009). Novel innovations are constantly in demand for pharmaceutical R&D to ensure overall cost-efficiency of the processes.

The quality-by-design (QbD) concept is in a vital role in pharmaceutical R&D (Csóka et al. 2018). QbD approach consists of many strategies during the multiple phases of NME development to avoid any pitfalls along the way. Selection of suitable molecules for screening, charting the therapeutic need for the molecule, identification of critical quality attributes and selection of critical process parameters are some of the strategies included in the QbD concept. Investing in early development is especially crucial to produce a solid ground to build on during later phases. Understanding material characteristics, effects of process parameters and the possibility of potential risks is of priceless value during the many phases of pharmaceutical R&D.

A suitable drug candidate should show safe and effective pharmacodynamic (PD) and pharmacokinetic (PK) profiles (Ferreira & Andricopulo 2019). In short, pharmacodynamics refers to drug potency and its affinity to the desired target. Pharmacokinetics can be described by ADMET-profile (absorption, distribution, metabolism, excretion and toxicity). Before absorption, the active pharmaceutical ingredient (API) must liberate from the drug product and achieve dissolved form. API liberation can be controlled by several means to achieve desired PK and PD profiles, if necessary. API is very rarely the only ingredient in a pharmaceutical product. Various excipients are used to reduce the potency of the mixture and to ensure the uniformity of content (Abrantes et al. 2016). However, acting as a filler or a solvent is not the only role of the excipients. They can have numerous effects, such as, adjusting pH in a solution or acting as a disintegrant in a tablet.

Out of all the possible dosage forms to choose from, tablets are still the most commonly used (Jivraj et al. 2000, Mohan 2012). Ease of use and rather simple manufacturing are some of the many advantages of tablets. Typical excipients in tablet formulations include fillers, disintegrants, binders, lubricants, glidants and colouring agents, to name a few examples. Tablets are often prepared by powder compression. When pressure is applied onto the powder sample, new bonds are formed between the particles and a coherent compact is formed. However, all solid materials have different mechanical properties, and adequate compact formation does not automatically occur during compression at one's convenience. For example, defects can occur due to excessive elasticity in the powder formulation.

Tableting simulators have been invented to aid the formulation scientist in tablet product development. These devices aim to mimic all stages of tablet production from die filling to ejection. Utilization of these devices allows the study of compressibility and compactibility of the mixture one tablet at a time. These methods are material-sparing as there is no need for large amounts of powder, unlike in actual tableting machines. Sparing resources is crucial as new APIs are often only available in small quantities. Tableting simulators are widely used in the pharmaceutical field (Rees 1972, Muñoz-Ruiz et al. 1997, Picker 2003,

Michaut et al. 2010, Abdel-Hamid et al. 2011, Akseli et al. 2013, Hirschberg et al. 2020, Khan et al. 2020). While tableting simulators are useful, they can still be costly and quite large. Also, they may require additional tinkering and adjustments to reliably pair them with an actual tableting machine (Neuhaus 2007).

This research project focuses on the development of a novel gravitation-based high-velocity compaction (G-HVC) method as an appropriate tool for the early phases of tablet product development. The primary aim was to see whether the mechanical properties of pharmaceutical powders could be analyzed by a simple experiment, where an object is dropped on a powder sample. This method was created to study specifically the mechanical properties of the solid material and to evaluate the tabletability of pharmaceutical powder formulations. The G-HVC method is designed to be material-sparing, simple and cost-efficient. Thus, it fits well in the modern environment of pharmaceutical R&D.

2 Review of the literature

2.1 Pharmaceutical powders

Powders are, one way or another, involved in a vast majority of pharmaceuticals. Thus, comprehensive knowledge of powder technology is a critical aspect in creating feasible pharmaceutical formulations. Powders can be administrated in their original, physical form as oral powders or dry powder inhalations, to name a few examples. More commonly, however, powders are processed further. For example, powders can be granulated, compacted into a tablet or dissolved in a liquid medium. Eventually, the active ingredient must achieve dissolved form to absorb and cause a systemic effect inside a body. In many cases, solid powders have various advantages over liquids in terms of handling and stability. However, handling of powders is not without its challenges. Tableting can fail due to insufficient powder flow, or incorrectly stored active pharmaceutical ingredient (API) can lose its effect due to oxidation, to name a few examples.

2.1.1 Solid-state forms and polymorphism

Like other solid materials, pharmaceutical powders may appear in several solid-state forms (Chieng et al. 2011). Crystalline materials consist of repeating unit cells, where molecules are arranged and oriented in a specific way. Materials that do not own such three-dimensional long-range order have their molecules arranged more irregularly and are known as amorphous. In general, it can be stated that both types of materials are prevalent among pharmaceutical solids. In addition, more than one type of repeating unit cell may exist, producing various forms for the same material. These forms are known as polymorphs, and it has been estimated that more than 50% of all organic materials can show polymorphism (Stahly 2007, Pindelska et al. 2017). Inclusion of solvents in the crystal structure is known as solvatomorphism (Chieng et al. 2011). Hydrates are solvates with water as the solvent. Single-phase solids that include more than one molecular or ionic compound, other than a solvate or a simple salt, are called cocrystals (Zhang et al. 2019).

Solid-state form of the material often has a significant role in pharmaceuticals. Insufficient aqueous solubility is a common problem with many APIs, and amorphous forms often show higher solubility and dissolution rate (Alonzo et al. 2010, Chieng et al. 2011). Amorphous structure allows improved mobility and a higher energy state, which also tends to cause physical instability. Consequently, amorphous material may revert to a stable or metastable crystalline form during manufacture or storage (Singhal & Curatolo 2004). Similarly, the material can undergo polymorphic changes from one form to another (Snider et al. 2004).

Polymorphism has a significant impact on physicochemical characteristics of a material (Suihko et al. 2001, Sinka et al. 2009, Chieng et al. 2011, Pindelska et al. 2017). Different polymorphs of the same material can have variance in density, solubility, melting point, colour and mechanical properties, to name a few examples. Differences in bioavailability

can hinder the effect of API or, on the other hand, promote toxicity. Therefore, it may be necessary to study a novel substance in "extreme" conditions, such as those with high temperatures or with various solvents included, to be aware of the possible polymorphic transformations.

Polymorphism also brings both challenges and opportunities in legal manners and patenting (Gupta et al. 2010). By patenting a specific polymorph after the original drug, the market exclusivity can be extended. This is a risky approach since the competitor may as well claim unpatented polymorph for themselves even though they would not own the rights to the original form. Therefore, screening for all possible polymorphs of a material in the early phase of pharmaceutical development is of vital importance.

2.1.2 Particle properties

Powder particle size and shape affect many phenomena during pharmaceutical processes and drug performance, for instance, powder flow, dissolution rate, content uniformity and drug disposition in dry powder inhalations (Sun & Grant 2001a, Rohrs et al. 2006, Patel et al. 2007, Shekunov et al. 2007, Abdel-Hamid et al. 2011, Zhang et al. 2011). Particle shape affects particle rearrangement and interlocking during compression. Rough particle surfaces also affect die-wall friction when tableting. A formulation consisting of a wide particle size range or density variation is susceptible to segregation and subsequent variance in content uniformity (Deveswaran et al. 2009). This obviously may lead to inaccurate dosing should the mixing be inadequate for the formulation at hand.

For direct-compression of tablets, the particle size typically varies between 100 and 200 µm (Shekunov et al. 2007). Strong interactions between small particles hinder sufficient powder flow, which is imperative for successful tableting. On the other hand, the inclusion of large particles in a tableting formulation may lead to insufficiency in content uniformity and reduced tensile strength (Rohrs et al. 2006, Abdel-Hamid et al. 2011).

Powder mixing is crucial in pharmaceutical manufacturing since different components in a mixture tend to advance towards equilibrium by segregating. Primary reasons for this are usually differences in particle size and density (Harnby 2000, Venables & Wells 2001, Deveswaran et al. 2009). Other reasons also exist, such as various interactions between the ingredients. The effect of gravity alone causes small particles to move and fill the voids between larger particles. Any vibration further promotes the movement of smaller particles under the larger ones and consequently lifting the large particles upwards. Other forces can also cause segregation, such as acceleration and deceleration during transport.

Nano-sized or micronized particles are in demand since many new APIs have poor aqueous solubility (Hu et al. 2004, Kipp 2004, Shekunov et al. 2007, Zhang et al. 2011). Decreasing the particle size increases the surface area, allowing more bonding to occur with water. However, these small particles can also form aggregates, due to high surface area to volume ratio, allowing remarkable interparticulate interactions.

While materials are generally more stable as solid particles compared to dissolved form, powder stability is still a crucial issue to consider. Due to physical transformations and chemical reactions, impurities are formed, which may decrease the potency of the drug,

disturb the stability of the formulation or produce toxic by-products (Roy 2002, Singhal & Curatolo 2004, Blessy et al. 2014).

2.2 Granulation

Insufficient powder flow affects adversely many phases of tablet production, such as mixing and die filling (Wu 2008, Sun 2010, Sun & Kleinebudde 2016). Direct compression is a process where the physical powder mixture is compacted in its original form. While this method can be simple and cost-efficient, powder segregation and poor powder flow may render the tableting process exhaustive or even unsurmountable. Granulation is a way to improve powder flow by increasing the particle size of the mixture. There are several different methods to produce granules, each with their advantages and disadvantages. Granulation also affects other properties besides powder flow, such as content uniformity and tabletability (Bacher et al. 2008, Arndt et al. 2018).

2.2.1 Dry granulation

Direct compression is the simplest method to produce a tablet as the physical mixture is compacted as is. When granules are required, dry granulation offers a rather effortless way for their production (Kleinebudde 2004, Herting et al. 2007). During the dry granulation process, a method known as roll compaction is utilized to compact the physical mixture into ribbon-form. The dry granules are then obtained by milling these ribbons. This method requires no liquid use or subsequent drying, which leads to a rather efficient and straightforward process. Also, dry granulation is often suitable for moisture and heat-sensitive substances. However, a significant number of fine particles deviating from the target particle size are likely to be formed during the process (Arndt et al. 2018).

One major drawback of dry granulation is the loss of tabletability due to roll compaction during ribbon production (Mitra et al. 2015, Grote & Kleinebudde 2018). Tabletability can be defined as a relationship between applied pressure during tableting and tensile strength of the produced compact (Sun 2011, Worku et al. 2017). The magnitude of pressure during roll compaction is therefore crucial, and higher forces tend to induce more significant loss of tabletability. There are several proposed mechanisms for this phenomenon, and one of the most commonly discussed is work hardening (Herting & Kleinebudde 2008). This term refers to dislocations in crystal lattice caused by plastic deformation during precompression. Caution must be exercised, though, when interpreting this hypothesis to pharmaceutical powders which are not often metals. Nevertheless, the larger particle size decreases the total bonding surface area during tableting, which has been shown to reduce tabletability, especially when the granules are hard enough to resist fragmentation during compression (Sun and Himmelspach 2006).

2.2.2 Wet granulation

Wet granulation is a method based on the inclusion of liquid solution and a binding agent in the powder mixture (Faure et al. 2001, Iveson et al. 2001, Suresh et al. 2017). Particles are bound together due to capillary and viscous forces, forming stable bonds upon drying. While this process requires more phases compared to direct compression or dry granulation, it can significantly improve the overall quality of granules. More reliable content uniformity and improved tabletability are some of the advantages that may be obtained utilizing this method.

High-shear granulation is carried out by enclosing the powder mixture inside a vessel, where it is agitated by a rotating impeller (Faure et al. 2001). Binder solution is sprayed into the mixture from the top of the vessel. The liquid is dispersed within the powder particles, forming so-called nuclei which grow further to form granules. High agitation forces prevent the overgrowth of granules since they will eventually fracture as the particle size increases (Iveson et al. 2001). However, excessive densification of the granules may occur if the process is continued for too long (Suresh et al. 2017). This eventually causes a phase inversion, where uncontrollable growth of agglomerates occurs. Therefore, time is an essential factor during high-shear granulation and more or less dense granules are expected to be produced.

Another commonly used wet granulation method is fluid bed granulation (Iveson et al. 2001, Šantl et al. 2011, Arndt et al. 2018). In this method, upward-injected air is used to fluidize the powder. At the same time, the binder solution is being sprayed from the opposite direction. Less dense granules are being formed with fluid bed granulation when compared to high-shear mixing. It has been shown that tabletability can be significantly improved by fluid bed granulation which may be due to their superior flowability, porous nature or surface properties (Šantl et al. 2011, Shi & Sun 2011, Van Den Ban & Goodwin 2017).

In conclusion, dry granulation is a simple and cost-efficient process, but wet granulation often produces granules with better properties for tableting. Moisture and heat-sensitive ingredients cannot be used during wet granulation, in which case, direct compression or dry granulation is often preferred. Furthermore, in some cases, loss of tabletability has been reported to occur due to wet granulation as well (Badawy et al. 2006, Shi et al. 2011). Therefore, the choice of the best possible method is always dictated by the material properties in a formulation.

2.2.3 Other granulation methods

Besides traditional roll compaction or wet granulation processes, other methods exist as well. Continuous wet granulation can be achieved utilizing twin-screw granulation. This type of device has two intermeshed, co-rotating screws, which drive the material forward in the system (Keleb et al. 2004, Seem et al. 2015). The screws have conveying and kneading sections on them. Added granulation liquid is also automatically distributed along the screws as they rotate, providing reliable and self-cleaning system. However, friction is to be expected between the kneading parts and the material, causing the temperature to rise

during the process (Vercruysse et al. 2012). As for the properties of granules produced, liquid-solid ratio plays a significant role in twin-screw granulation. An increase in liquid content promotes the production of denser and more spherical granules, due to enhanced compaction properties. One drawback of twin-screw granulation is that producing granules of desirable qualities may require some trial and error. This method tends to be sensitive to formulation properties and different variables in the process, leading to the need for careful optimization.

Granulation liquid can also be added as a foam (Cantor et al. 2009, Thompson et al. 2012, Tan et al. 2013). It has been reported that less amount of binder is required in a foam form, producing a drier environment. Foam granulation may decrease friction during the twin-granulation process, affect the mechanical properties of granules and provide more uniform granules when compared to traditional wet granulation.

Melt granulation is a process where powder particles agglomerate through the use of binding material that has a low melting point (Passerini et al. 2010). The substance is added to the powder in a molten form or its original powder form, given that the process itself causes sufficient temperature rise for the material to melt. Molten binder reverts to solid after cooling, allowing granules to remain intact. In practice, this method can be utilized as an alternative to wet granulation and even similar devices, such as high-shear mixer, fluidized bed or twin-screw granulator, can be used (Walker et al. 2006, Passerini et al. 2010, Măsić et al. 2012, Monteyne et al. 2016). The absence of solvents can be a considerable advantage when utilizing hot melt granulation. Also, controlled-release granules can be rather easily produced with suitable melting binders, such as polyethylene glycols. One must be aware that the molten binder can effectively cause unwanted reactions as well, should an interaction exist between the binder and the other ingredients. The absence of evaporating solvent may also cause low-porosity granules to be produced, possibly hindering the wanted intrusion of water into the granules, when inside the GI tract (Walker et al. 2006).

2.3 Tableting and mechanical properties of powders

Adequate powder flow is required to ensure proper die filling during tableting (Patel et al. 2006). After filling the die with the powder, the pressure is applied by forcing the material in a space between two moving punches. Within that space, depending on mechanical properties of the powder mixture, a coherent compact may be formed if sufficient and permanent bonding occurs between the powder particles. Several types of tablets exist, depending on the targeted pharmacokinetic profile (Allam et al. 2011, Cascone et al. 2011). Conventional or immediate-release tablets are produced when the desired properties are quick disintegration of the compact and fast dissolution of the API. Extended-release tablets are prepared when the API is meant to liberate and dissolve slowly or evenly for a longer period of time, allowing a prolonged effect. In some cases, the API is released from the compact in certain sections of the GI tract, usually triggered by changes in pH. These preparations are known as delayed-release tablets. The absorption of the substance is caused by active transportation pathways or pH-dependent passive mechanisms in the GI tract.

While gastric pH is ideal for many substances in terms of absorption, the large surface area of the small intestine is usually the most effective location for the APIs to absorb and consequently cause a systemic effect. In some cases, tablets are used for local treatment as well, for instance, in the buccal cavity or colon.

2.3.1 Particle bonding and compact formation

When pressure is applied on the powder bed, particles rearrange, fragment and deform, allowing more surface area with bonding potential to be in contact between the particles (Li et al. 2004, Patel et al. 2006). Several mechanisms have been proposed for the particle bonding, such as Van Der Waals bonding, electrostatic forces, hydrogen bonding, local melting and mechanical interlocking of the particles. The presence of moisture is of importance as dry powders often show poor compactibility (Nokhodchi 2005). Local melting, on the other hand, is a consequence of high pressure and temperature rise at the particle contact points. Mechanical interlocking refers to a phenomenon where particles become geometrically entangled, like paper clips in a container.

Bonding requires energy which is subsequently stored within the bonds (Busignies et al. 2006, Buckner et al. 2010a, Buckner et al. 2010b). High bonding energy generally leads to compacts with high tensile strength. Sufficient hardness is required to some degree for every tablet as they must endure further manufacturing processes, such as coating, packing and transport. The amount of energy transferred from the compression process into the bonds is highly material-dependent as some ingredients show more energy intake than others.

2.3.2 Powder consolidation and elasticity

Under pressure between the tableting punches, the powder particles rearrange, deform and fragment so that the particles fill the available space as comprehensively as possible (Adolfsson & Nyström 1996, Patel et al. 2006). Fragmentation is a phenomenon where the original particle breaks down to smaller ones. Roughly put, there are three types of fragmentation (Hansen & Ottino 1997). Abrasion grinds small pieces off particle surfaces, and cleaving fragmentation ideally splits the particle into half. Destructive fragmentation takes place when the original particle fragments completely into smaller pieces. The specific mechanism of fragmentation is typically more or less a combination of all these types. High pressure may cause destructive fragmentation, while low pressure may only cause abrasion. One can imagine this by thinking what would occur if one would hit a chunk of sugar with a hammer, with varying forces. Large particle size and irregular particle geometry may also favour the occurrence of fragmentation. In general, the propagation of a crack and fragmentation are a consequence of an atomic level shift in the crystal lattice, producing a dislocation (Cleveringa et al. 2000, Zhu et al. 2004). Through repulsive and attractive forces, new low-energetic balance state is formed, which then may produce a crack in the material. In other words, the fragmentation is a consequence of the inability to deform in a way to prevent the formation of dislocations in the material.

When particle deforms under pressure, it changes shape reversibly until the elastic limit or yield point of the material has been reached (Patel et al. 2006, Chattoraj et al. 2010, Ayorinde et al. 2013). If the applied pressure exceeds the elastic limit, the material will begin to yield and will eventually fragment if the fracture pressure is exceeded (Fig. 1). Plastic deformation refers to the type of yield, where the particle changes shape permanently and remains in its new form. Elastic recovery occurs as the particle is unable to assume a new form and reverts to its original form. Plastic deformation is a time-dependent phenomenon and may not occur if compression speed is high enough. Fragmentation occurs if sufficient pressure has been applied, regardless of compression speed. It is said that the compression mechanics of the material are a combination of all these phenomena and every material can show fragmentation, plasticity and elasticity to some degree.

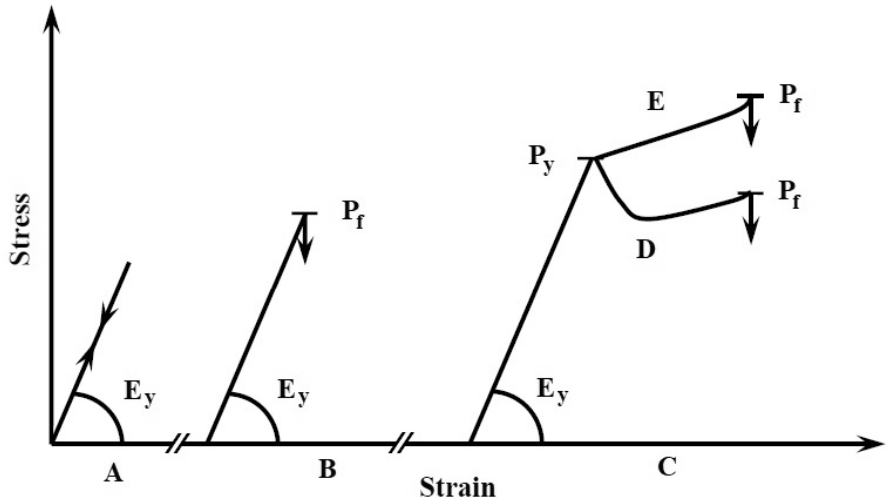

Figure 1. Stress-strain graphs for different materials. A) Reversible elastic deformation, B) fragmenting behaviour, C) plastic behaviour, D) typical plastic flow, E) work-hardening behaviour. E_y is Young's modulus, P_f is the fracture pressure, and P_y is the yield pressure.

Elastic recovery can be divided into two phases. Spontaneous elastic recovery refers to the portion of deformation below the yield point, and the viscoelastic recovery occurs to some degree when the yield point has been exceeded (Haware et al. 2010). Therefore, the total elastic recovery of the compact is the sum of the two. All materials show elasticity to some degree, while its magnitude can vary significantly between materials (Picker 2001). Same can be stated for plasticity and fragmenting behaviour as well. Plastic deformation is a time-dependent phenomenon, and consequently, high-speed compressions favour elastic or fragmenting behaviour over plastic deformation (Akande et al. 1998, Ayorinde et al. 2013). The absence of moisture may also hinder plastic behaviour as water is often in a crucial role in bond formation (Nokhodchi 2005).

2.3.3 Successful tableting – The impact of mechanical properties in a mixture

Knowing the mechanical properties of the materials is crucial when designing a feasible tablet formulation (Patel et al. 2006). Excessive elasticity may cause defects, such as lamination or capping, in a tablet or completely prevent coherent compact formation (Wu et al. 2008, Akseli et al. 2013, Furukawa et al. 2015 Sarkar et al. 2015, Paul & Sun 2017). Capping refers to a defect, where the top or the bottom of the tablet separates and is cut off. Lamination is a similar horizontal defect but affects the main body of the tablet. While excessive elasticity is a major problem, an overly plastic formulation may turn out to be too hard, which may hinder disintegration and subsequent dissolution of the API inside the GI tract. As a rule of thumb, it is often reasonable to include ingredients with different mechanical properties in a formulation to prevent some of these pitfalls. It is also of importance to keep in mind that not only mechanical properties dictate the performance of the tablet. Different excipients have wide mechanisms of action such as binding or disintegrating effect, which may render some other properties, even the unwanted ones, negligible.

One common and unpleasantly hidden bane in tablet production is fracturing of the compacts during storage. This is caused by stored elasticity in the tablets, which is slowly recovered over time (Van Der Voort Maarschalk et al. 1996, Van Der Voort Maarschalk 1997, Anbalagan et al. 2017). This phenomenon can occur in mixtures where the plastic or fragmented and rearranged materials cause the elastic material to be trapped inside the structure. Consequently, the compact appears feasible right after production but is broken down during transport or storage. Excessive elasticity should, therefore, be considered a red flag even though no immediate effects could be seen. As an example, when compressing binary mixtures of plastic and elastic material with varying compositions, points known as percolation thresholds may be found (Kuentz & Leuenberger 2000, Amin & Fell 2004). At these points, the compressibility is suddenly changed due to the properties of one material overcoming another. However, producing compacts at such percolation threshold could cause problems later due to hidden elasticity. Consequently, one could steer away a bit to the safer side of the percolation threshold to avoid this.

2.3.4 Mechanical properties of some common pharmaceutical ingredients – Examples

Mechanical properties of materials are always condition-dependent to some degree, but in a typical tableting setting, each material tends to behave in a certain way. Lactose and glucose are primarily fragmenting materials with low yield pressure (Eriksson and Alderborn 1995, Juppo et al. 1995, Juppo 1996, Lamešić et al. 2017). Exceptions also exist, as amorphous lactose is capable of showing plastic behaviour (Berggren et al. 2004). In general, rigid crystalline materials are more prone to fragmentation than amorphous materials. In some cases, the yield pressure of the material is so high that little to no change occurs in the particles during compression. Such is the case with dicalcium phosphate with

a yield pressure reported to be over 300 MPa (Doldán et al. 1995, Nicklasson et al. 1999). In comparison, yield pressure for lactose is roughly 100-200 MPa (Eriksson and Alderborn 1995).

Microcrystalline cellulose (MCC) could be considered as one of the "jacks-of-all-trades" in tablet formulations. Not only is it an excellent filler but also has a binding and disintegrating effect (Bolhuis & Armstrong 2006, Thoorens et al. 2014). MCC shows remarkable plasticity but is also elastic (Buckner et al. 2010b). These properties may be the reason why MCC resists work hardening quite well during consecutive compressions, which is required for producing decent dry granules, for example. Loss of tabletability due to precompression may be an issue with some of the plastic ingredients, and it has been reported to occur with MCC as well (Sun & Himmelspach 2006, Sun & Kleinebudde 2016). For example, theophylline, an API used in tablets for asthma treatment, shows excellent compressibility and compactibility (Suihko et al. 2001, Chang & Sun 2017). However, for the same reason, materials like theophylline may lose their bonding potential if too much pressure is applied during precompression. Knowing these aspects is crucial when producing a mixture to ensure proper compactibility in the tableting phase.

All materials show elasticity to some degree. Some materials, such as different starches, show remarkable elastic recovery during tableting (Jivraj et al. 2000, Anuar & Briscoe 2009). Starches are generally good disintegrants and are often used in tableting formulations. Elasticity is often something of an obligatory nuisance to be present in tablet formulations, as other materials are usually required to overcome its effects to produce a decent compact.

2.4 Mathematical models for the deformation and tabletability of powders

When producing tablets, both compressibility and compactibility of the powder mixture have to be considered. Compressibility depicts the volume reduction occurring in the material during compression, whereas compactibility refers to the ability to produce coherent and sturdy compacts from the powder (Leuenberger & Rohera 1986, Jain 1999). Several mathematical models have been used to study these issues, some of which are presented in this section.

2.4.1 Powder deformation and compressibility

2.4.1.1 Heckel's plot

Change in sample porosity during compression can be calculated by utilizing Heckel's plot:

(1) $$Ln[1/(1-D_r)]=KP+A,$$

where D_r is the relative density of the in-die sample at each pressure value, P, during the compression (Heckel 1961, Sonnergaard 1999, Denny 2002). Pressure does not remain constant during powder compression, but increases during the compression phase until maximum pressure has been reached and decreases back to zero during the decompression phase. Therefore, two values depicting powder density are created for each pressure point, one for the compression phase and one for the decompression phase (Fig. 2). (Ideally, however, there is only one point at maximum compression pressure.) K and A are used as a coefficient and a constant to define the slope during the linear section of the compression phase. Steep slope refers to the material being easily compressible as less pressure is required to induce higher density change in the sample. Thus, the mean yield pressure, P_y, is calculated as the reciprocal of K. The initial part of the curve (Fig. 2a) depicts the rearrangement and fragmentation of the powder. It is followed by the linear deformation phase (Fig. 2b), which is a result of plastic deformation and, in some cases, additional fragmentation. As the compression cycle reaches the maximum pressure point, the sample may still undergo work hardening (Fig. 2c). Elastic recovery can be seen during the decompression phase (Fig. 2d) as the density of the sample decreases along with the pressure decrease.

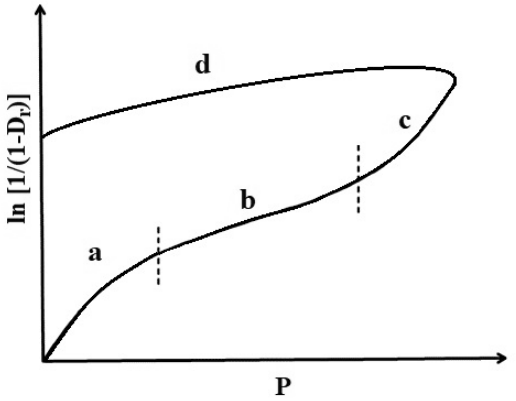

Figure 2. Representation of a Heckel's plot. a) Rearrangement phase, b) linear deformation phase, c) hardening phase, d) elastic recovery phase. P is compression pressure and D_r is relative density.

Relative in-die density, D_r, is defined as:

(2) $$D_r=D_a/D_t,$$

where D_a is the apparent density of the sample in-die, based on its weight and dimensions, and D_t is the true density of the material.

While Heckel's plot has been used widely in the pharmaceutical field, it was initially derived for metals. This has spawned criticism in use for pharmaceutical, often organic, powders as results have had significant variance (Sonnergaard 1999). Sun and Grant

(2001b) reported that caution should be exercised if the porosity of the sample is under 0.05 since the porosity value, as depicted in Heckel's plot, will change dramatically. They also reported that low elastic modulus of the material causes deviations in the results. Elastic materials, which are not uncommon in pharmaceutical formulations, may show results deviating from the real value. Thus, the results obtained by utilizing Heckel's plot should always be carefully interpreted. Attempts have been made to modify Heckel's plot to improve its reliability in the pharmaceutical field. One such example is the consideration of yield pressure being pressure-dependent during tableting and the addition of a suitable correcting term in the original Heckel's equation (Denny 2002).

2.4.1.2 Young's modulus and elastic recovery

Elastic deformation occurs immediately during decompression phase when the compression pressure decreases and may continue after the pressure has been completely lifted (Haware et al. 2010, Mazel et al. 2013, Keizer and Kleinebudde 2020). Later elastic recovery occurs immediately after the tablet is ejected from the die but may continue for an extended period of time during storage.

Material elasticity can be observed from the stress-strain relationship (Jain 1999, Patel et al. 2007, Katz & Buckner 2013). Stress refers to the force applied to the sample, and strain denotes the dimensional change as a consequence of given force. Close to zero stress and strain, the linear portion of the stress-strain curve can be found. The elasticity factor, Young's modulus, can be observed from this portion by Hooke's law:

$$F=E_y\varepsilon, \quad (3)$$

where E_y is Young's modulus, F is applied stress and ε is the deformation strain. Thus, materials with higher Young's modulus are stiffer than those with low modulus.

During uniaxial in-die powder compression, the difference between the sample height during and after compression shows the magnitude of elastic recovery:

$$ER=100(h_a-h_c)/h_a, \quad (4)$$

where ER is relative elastic recovery, h_c is the lowest powder bed height during the compression and h_a is the powder bed height after the compression. There are different variations of this equation, for instance, where the amount of recovery is related to the lowest height, instead of the height after compaction (Jain 1999, Picker 2001, Haware et al. 2010, Osamura et al. 2016). Also, elastic recovery can be observed in-die, when it can be referred to as immediate in-die elastic recovery. After ejection, when the compact is released from the constraints of its "steely prison", it will show more elastic recovery. Also, elastic recovery can occur for a substantial time after ejection. Therefore, when comparing elastic recovery values from different sources, it is of importance to double-check the calculation method in use.

2.4.1.3 Plasticity indicators

Plastic deformation occurs after the point known as the elastic limit has been exceeded in the stress-strain curve. This type of deformation is time-dependent and may consequently occur only partially during high-speed tableting. Plasticity has its limit, too, if further stress is applied, leading to propagation of a crack and fracturing of the material. Permanent deformation is the consequence of the formation of durable particle-particle bonds during compression.

Since plastic deformation is time-dependent, differences in punch speed can be utilized to study plasticity (Ruegger & Çelick 2000, Michaut et al. 2010). Consolidation of fragmenting materials remains rather unchanged when different punch speeds are used, given that the pressure is kept constant. If the material shows remarkable deformation during low-speed compressions but poor deformation during high-speed compressions, plasticity may be the dominant factor of consolidation.

Plasticity can be observed and quantified by utilizing strain rate sensitivity calculus:

$$SRS=100(P_{yh}-P_{yl})/P_{yh}, \quad (5)$$

where *SRS* is strain rate sensitivity, P_{yh} is yield pressure at highest compression speed, and P_{yl} is yield pressure at the lowest compression speed. If no remarkable change in yield pressures can be found, the equation gives out low value, indicating low plasticity in the sample (Roberts & Rowe 1985, Jain 1999, Patel et al. 2007, Katz & Buckner 2013).

Stress relaxation can be studied to observe the time dependency of plastic behaviour (Van Der Voort Maarschalk 1997, Jain 1999, Anbalagan et al. 2017). The upper punch is kept stationary on top of the powder sample, and pressure is increased until it reaches the target value (which varies, depending on material). During the holding period, the upper punch pressure decreases as some of the energy is consumed in plastic flow and particle bonding. Stress relaxation can be quantified by various methods, one of them being Maxwell's model:

$$\ln\Delta F=\ln\Delta F_0-kt, \quad (6)$$

where ΔF is the remaining compression force at time t and ΔF_0 is the compression force at time zero. At time zero ΔF and ΔF_0 are of equal value, and ΔF starts to decay as plasticity occurs. Slope k then indicates the rate of this phenomenon.

2.4.1.4 Fracture toughness

When applied pressure, P, exceeds the yield pressure, P_y, the material deforms and, at some point, undergoes fragmentation. Roberts and Rowe (1989) described fracture toughness, R, as:

$$R=[K_{Ic}^2(1-\nu^2)]/E_y, \quad (7)$$

where K_{Ic} is the critical stress intensity factor, which describes at what point the magnitude of stress is sufficient enough to cause the propagation of a crack. E_y is Young's Modulus, and v is Poisson's ratio. High values of K_{Ic} indicate high resistance to fragmentation. Several equations for fracture toughness exist as each is utilized to describe different types of materials and conditions (Zhu & Joyce 2012).

2.4.1.5 Force-displacement plot and compaction energy

Energy consumed in compact formation is often calculated utilizing the force-displacement curve (Fig. 3) (Antikainen & Yliruusi 2003, Aburub et al. 2007, Buckner et al. 2010b). By monitoring the upper punch movement and compression force, a plot can be drawn where the area under the curve (AUC) of the plot depicts the energy transferred into compact formation. Compaction energy is often considered a decent indicator for subsequent tablet hardness. This plot can also be used to evaluate elasticity, plasticity and fragmentation, to some extent. The energy value obtained by this method is not free of errors, though. The energy consumption in deformation of the machine parts and die-wall-friction are some of the phenomena included in the result. Since errors are possibly present in both, force and displacement measurements, multiplication of the total error has to be accounted for as well.

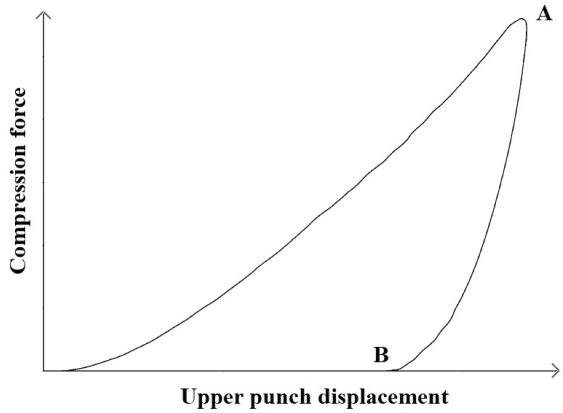

Figure 3. Representation of a force-displacement graph. A) Maximum displacement and B) final displacement.

Additionally, various other methods exist for the examination of energetics involved in powder compaction (Coffin-Beach & Hollenbeck 1983, Çelik 1992, Wurster et al. 1995, DeCrosta et al. 2000, Mangal et al. 2016). As an example, one of these is the thermodynamic analysis, which is based on measuring the temperature rise during powder compaction. When the specific heat of the sample and the surrounding environment is known, the heat of compaction can be approximated. This, in turn, allows the calculation of internal energy change in the system, depicting the amount of work consumed during powder compaction.

2.4.2 Compactibility measurements

2.4.2.1 Tensile strength

Crushing strength is measured by compressing a tablet sample until breakage, with a tablet hardness tester (Leuenberger & Rohera 1986, Sonnergaard 2006). The value obtained is simply the magnitude of force required to break the tablet, and the method completely ignores the tablet size and geometry. Therefore, calculating tensile strength is more reliable when evaluating tablet hardness:

$$\sigma_t = 2F_c/(\pi dH), \quad (8)$$

where F_c is crushing strength, d is tablet diameter, and H is tablet height. Therefore, larger tablets have weaker tensile strength, even if the crushing strength was similar to tablets of smaller size. This is a more suitable indicator for actual tablet hardness. However, some errors are present with this method as well, since some irregular tablet geometries or variations in tablet homogeneity affect the results, to name a few factors. Since tablets of many different shapes exist, there are also various derivations of the classic tensile strength equation (Pitt & Heasley 2013, Shang et al. 2013, Razavi et al. 2015).

2.4.2.2 Compression force vs tensile strength and deformation hardness

To evaluate a formulation for its ability to form strong tablets, a comparison between compression force and tensile strength can be made (Sonnergaard 2006, Sun 2011, Osei-Yeboah et al. 2016). Tableting speed should be kept constant as compression force is varied. The graph can provide useful information about the compression pressure range, which could be suitable for the formulation at hand. The slope of the curve is a direct indicator of the performance of the formulation to produce sturdy tablets.

Another way to evaluate compactibility is to compare compression pressure to deformation hardness (Leuenberger & Rohera 1986):

$$P_d = P_{max}(1-e^{-\gamma P D_r}), \quad (9)$$

where P_d is deformation hardness, P_{max} is theoretical maximum deformation hardness, γ is compression susceptibility, P is applied pressure and D_r is relative density. P_{max} and γ are quantified from the equation. When applied pressure is increased towards infinity, deformation hardness approaches its theoretical maximum. Low P_{max} values may predict poor compactibility as this value cannot be further increased by adding compression pressure. Parameter γ depicts the impact of applied pressure and can be seen as an indicator for compressibility as a high value of γ leads to a sharp decrease in porosity. This equation

is based on the hypothesis of available bonding points within the sample during tableting. As P_{max} is reached, the available bonding points are considered zero.

2.5 Tableting machines and simulations

Nowadays, tablets can be produced with a remarkable output, exceeding one million tablets per hour (Kremer 2006). While modern tableting machines are more efficient than the traditional ones, different types of devices share some standard features (Palmieri et al. 2005, Mohan 2012). First, the powder is fed from the hopper into the die. Next, the powder is forced between two compressing punches with a certain pressure. Lower punch serves as the bottom of the die and moves up while the upper punch moves down inside the die. Finally, the lower punch moves further up, ejecting the tablet. Tablet size can be controlled by changing the die diameter and maximum positions of the punches. In addition to classic methods, tablets can also nowadays be prepared by ultrasound-assisted compression, hot-melt extrusion and even 3D-printing, to name a few examples. (Rowe et al. 2000, Baronsky-Probst et al. 2016, Millán-Jiménez et al. 2017, Puri et al. 2017, Casas et al. 2019, Ibrahim et al. 2019, Jennotte et al. 2020). These methods are not discussed any further in this work.

2.5.1 Eccentric machines

Traditional eccentric tablet presses cannot compete with modern machines in terms of tablet output. These machines are also known as “single-punch” or “single-station” devices, and only one tablet is being compacted at a time. The mechanism of action could be described as “hammering” since the lower punch is stationary while the upper punch applies the compression force. Eccentric machines are powered by hydraulic pressure, and the mechanism of action is straightforward with a single set of punches. While eccentric machines are not generally competent in tablet manufacturing anymore, they can still be of use in research and development purposes (Krumme et al. 2000, Antikainen & Yliruusi 2003, Palmieri et al. 2005, Michaut et al. 2010).

2.5.2 Rotary machines

In rotary tableting machines, there are multiple sets of punches in a rotating system. Movement of the punches is directed by rollers and cams, allowing punch displacement up or down as required (Charlton & Newton 1986, Palmieri et al. 2005, Michaut et al. 2010). This type of system is sometimes referred to as “accordion-type”, sort of resembling the musical instrument. Therefore, multiple tablets can be handled at one time, significantly increasing the tablet output to over one million units per hour. Dwell-time, which refers to the time window, when the punches are in contact with the powder, can also be extended by changing the distance between rollers. This is an important feature, especially for permanent plastic deformation, which requires time to occur.

2.5.3 Tableting simulators

When designing a tablet formulation, reliable estimate for the tabletability of the composition has to be established. Running tableting machines tend to require a large amount of powder to ensure proper die filling. Consequently, mere testing of a formulation may prove to be a bit too material-consuming, especially with new APIs, which are usually not available in large amounts. Single-stationed, eccentric presses and rotary machines have been used for test formulations as the die can be filled manually and tablets can be produced one at a time. However, to monitor different parameters of the compressions reliably, somewhat exhaustive tinkering may be required. Furthermore, eccentric-type compression rarely depicts an actual tableting situation, which is usually carried out using a rotary machine.

Tableting simulators were created to imitate tablet production with minimal material usage, one tablet at a time from die filling to ejection. One could assume that such a simulation is a rather recent approach to preformulation, but the idea and methods have been around since the 1970s (Rees 1972). Modern simulators resemble a rotary tableting machine in their mechanism of action, albeit the circular position of the punches is typically set in a straight line. *Stylcam* by Medelpharm and *The Presster* by Measurement Control Corporation are some of the simulators available in the market, which have been used in research (Picker 2003, Michaut et al. 2010, Abdel-Hamid et al. 2011, Akseli et al. 2013, Hirschberg et al. 2020, Khan et al. 2020). Several tableting conditions such as compression pressure, dwell-time or ejection force can be controlled with tableting simulators, providing useful information for the scale-up of the production.

While tableting simulators are undoubtedly useful tools during preformulation phase, caution should be exercised to some degree, when interpreting the results (Bateman et al. 1989). Still to this day, these devices can be considered expensive and completely accurate simulations are near impossible to carry out (Jain 1999). The simulator may have to be paired with each tableting machine to prevent errors, which can be exhaustive work (Neuhaus 2007). Tableting conditions vary depending on which machines are in use, and the data obtained from a simulator always requires further interpretation, more or less. Regardless, tableting simulators have solidified their place in pharmaceutical development and are extensively used in the field.

3 Aims of the study

The aim of this study was to develop a straightforward and cost-efficient method to evaluate the mechanical properties and tabletability of pharmaceutical powders. The objective was to produce a novel technique, which could be utilized effortlessly during the early stages of pharmaceutical R&D. The device constructed for the studies was planned to be significantly smaller than a traditional tableting machine or a simulator.

More specifically, the objectives of this dissertation were to:

- evaluate the applicability of the method, and to study two different materials to demonstrate the capabilities of the method **(I)**;
- evaluate the mechanical properties more comprehensively for a wide range of materials with two different energy input levels to further display the differentiating potential of the method **(II)**;
- prove the practical relevance of the method by estimating the compactibility of mixtures, and by enhancing the compaction energetics calculus to evaluate the tabletability of actual tablet formulations **(III)**.

4 Experimental

4.1 Materials

A total of 12 different materials was studied, including Amioca powder TF (National Starch), anhydrous calcium hydrogen phosphate (Merck), anhydrous glucose Ph. Eur. (Yliopiston Apteekki), Avicel PH-102 (FMC BioPolymer), Avicel PH-200 (FMC BioPolymer), dicalcium phosphate dihydrate (DCP) (Chemische Fabrik Budenheim), Methocel (DOW Chemical Company), Pharmatose 80M (DMV-Fonterra Excipients), Pharmatose 200M (DMV International), Starch 1500 (Colorcon), theophylline Ph.Eur./USP (BASF) and Vivapur 101 (JRS Pharma). Magnesium stearate Ph. Eur. (Yliopiston Apteekki) was used as a lubricant in some formulations and it was also mixed with technical grade acetone producing 5 w/w (%) mixture to lubricate the device. Amioca powder is a type of starch, Avicel and Vivapur are different grades of MCC, Pharmatose is lactose monohydrate and Methocel is hydroxypropyl methylcellulose (HPMC). Materials were selected to present a wide range in terms of mechanical properties.

4.2 Methods

4.2.1 Gravitation-based high-velocity compaction (I-III)

Gravitation-based high-velocity compaction method was developed to study the mechanical properties of powders and to evaluate tabletability of samples. G-HVC method is based on a freely falling weight, which is being monitored by a displacement laser. The movement pattern of the falling weight is analyzed as it collides with the punch, leading to powder compression.

4.2.1.1 Device structure

A setup constructed for G-HVC method consisted of a steel bar with a length of 1 m and a total weight of 6.27 kg, mounted to a rigid frame and held in place mid-air by a magnet (Fig. 4). The magnet could be deactivated through the use of power supply, allowing the bar to fall. Adjustment bolt on top of the system could be rotated to set the target falling height. Between compressions, the bar was placed on a safety latch. Two Teflon-coated bearings were used to minimize the friction and to ensure strictly vertical movement of the bar. Upper extension piece was installed to restrict torsional and rotational motion. A Teflon-coated scale was attached on the top side of the frame to measure the falling height of the bar. Customized circular punches with a height of 18 mm and diameters of 4 mm and 8 mm, with corresponding dies were in use. The customized die, weighing 2.71 kg, could be

dismantled into three parts to allow the removal of the compact inside the die. It is of importance to note that the bar and the punch were not attached in this setup, but were two separate parts. This was one major deviation from an actual tableting machine, but this feature was imperative for the method to function.

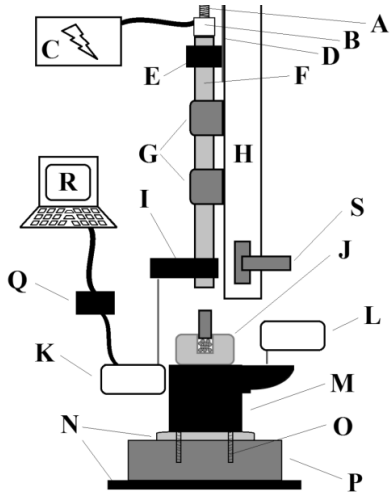

Figure 4. Schematic representation of the gravitation-based high-speed compaction device. A) Adjustment bolt, B) magnet, C) power supply, D) falling height scale, E) upper extension piece, F) falling bar, G) bearings, H) main frame, I) lower extension piece, J) punch and die, K) bar displacement sensor, L) base displacement sensor, M) anvil, N) rubber sheets, O) attachment pin, P) concrete brick, Q) data acquisition controller, R) laptop and S) safety latch. (Reprinted with permission from publication I.)

A steel anvil with a weight of 49.0 kg was used as the base of the system, and the customized die was attached to it by three bolts. The anvil was attached to a concrete base with a weight of 11.5 kg with four attachment pins, resulting in a combined weight of 63.21 kg for the base of the system, including the die. A rubber sheet was placed under the base to increase friction and to hinder the horizontal movement of the base due to compressions. There was also another rubber sheet between the anvil and the concrete brick. This ensured a tight attachment and prevented the brick from fracturing. A massive base was required to minimize its movement due to compressions since it had to withstand remarkable forces. As an anecdote, before the rubber sheet was set under the base, it would move remarkably during each compression. This was immediately noticed as the bar would no longer hit the centre of the punch during consecutive compressions. The anvil was made of decarbonized steel, and other machine parts were made of hardened steel (HRC 60-64).

Two high-accuracy laser displacement sensors (Keyence LK-H087, Keyence Corporation of America, Itasca, Illinois, USA) were in use to record the movement of the falling bar and the deformation wave in the base. The laser was pointed at the lower extension piece in the bar to record its displacement. The deformation wave of the base was recorded off-centre of the anvil to prevent equipment damage. Lasers were connected by

cables to a data acquisition controller, Keyence-G5001P (Keyence Corporation of America, Itasca, Illinois, USA). The controller was connected to a computer with the required software, Keyence LK_H3 (Keyence Corporation of America, Itasca, Illinois, USA), in use. The sensors were used with fixed settings throughout the whole study, with a detection accuracy of 1 µm and a sampling rate of 20 kHz (1 data point per 50 microseconds). With these settings, the laser range was 36 mm, which was sufficient for this study. The measurement window was 3.75 seconds, during which 75000 data points were recorded.

4.2.1.2 Principle of action

All data acquired with G-HVC method is based on distance as a function of time. First, the zero point of the bar distance is set by setting the bar on top of the empty die. The zero value then depicts the bottom of the die and, consequently, the distance value represents the in-die powder bed height during compression. The sample is measured and applied inside the lubricated die. The punch is then set in the die, on top of the powder. Next, when the target falling height has been adjusted with the bolt, the bar is lowered to be held in place only by the magnet. As the power supply is turned on, the magnet deactivates, and the bar starts to fall, with an acceleration near Earth's gravity, approximately 9.7 m/s^2. When the bar hits the punch, the powder compression begins, and the bar starts to decelerate. After reaching the maximum displacement point, a springback of the bar occurs and the sample recovers elastically. After this, the bar falls and collides again with the powder and may undergo more subsequent springbacks. When the event is over, the bar rests on the punch and final displacement level has been reached. Since all applied energy is not consumed in powder compaction and springback, a deformation wave can be observed in the base of the system, which is also monitored by a displacement sensor. Theoretically, if all applied energy were to transfer completely into compact formation, no springback or deformation wave would be detected. In practice, this is never the case. The outcome of the compression event is ultimately only dictated by the properties of the powder, which can "freely" resist deformation under the falling weight. This differs from traditional tableting machines, which compress the samples into predetermined volume with a predetermined pressure and contact time.

The compression cycles can also be carried out without a sample inside the die, to detect springback and deformation phenomena specifically. It is crucial to note that the displacement sensor follows the movement of the bar and not the punch. However, whenever the acceleration deviates from the near gravity 9.7 m/s^2, the bar is in contact with the powder and depicts the in-die powder height (Fig. 5).

During experiments, the powder samples were compressed consecutively five times, in triplicate. The falling height varied from 7 mm to 40 mm, producing a maximum vertical speed of 900 mm/s, approximately. Two flat-faced punches with diameters of 4 mm and 8 mm were in use. Sample size varied from 20 mg to 200 mg. Thus, both actual size compacts and smaller samples were examined. In one part of the experiment, a precompression was carried out by lowering the bar on top of the sample for 60 seconds before the set of five compressions (III).

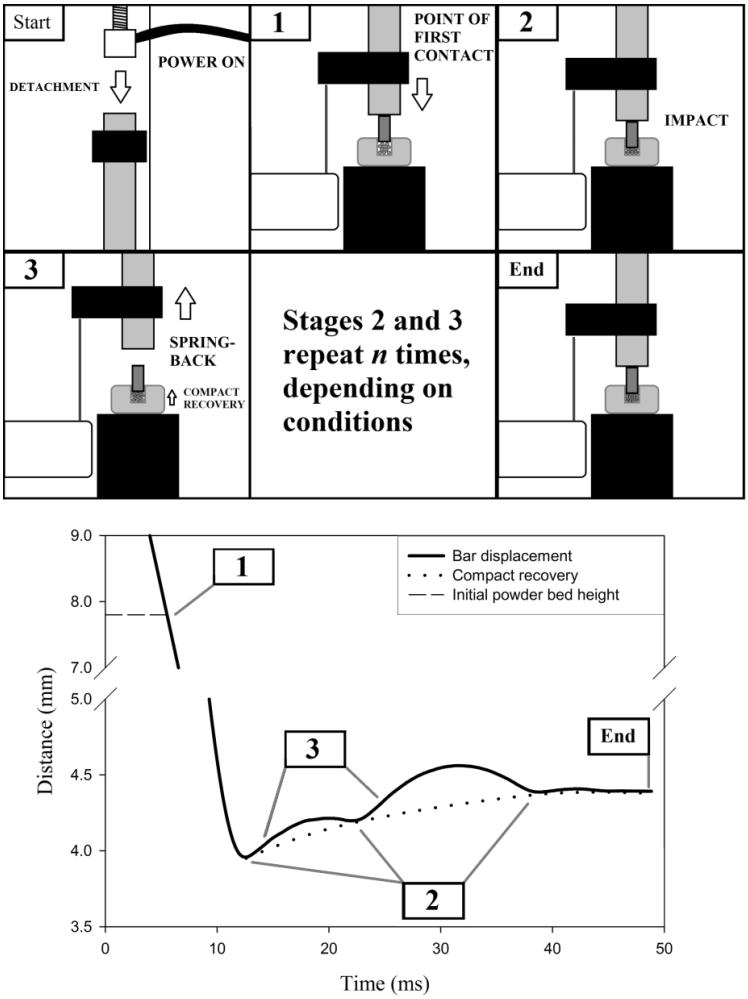

Figure 5. Stages of powder compaction with the G-HVC method. (Reprinted with permission from publication I.)

4.2.2 G-HVC data analysis (I-III)

4.2.2.1 Overview of the calculation program (I-III)

The raw data acquired from the displacement sensors consists of a set of paired values. The first value indicates the time step, which was set at 50 µs in this work. The second value indicates the distance of the monitored object. Two datasets were produced at each measurement since both the falling bar and the base were monitored. Acquired distance-time plots were then derived further utilizing a unique program coded with MATLAB

(Mathworks Inc, Natick, Massachusetts, USA). The basic principles of this program are explained in this section. The full code is presented in *Supplementary information*.

4.2.2.2 Displacement, velocity and acceleration (I-III)

The raw data indicates distance as a function of time and does not initially require any smoothing. Velocity and acceleration can be derived from this data as the first and second derivative. Smoothing was necessary at this point, however, to reduce noise caused by the derivation. Savitzky-Golay filtering was used for the displacement plot, and slightly different parameters were used throughout the study. Quadratic polynomial fit (I-III) and a window size of 7 (I) or 21 (II-III) were in use. Filtered distance-time plot was then derived to obtain the velocity data, which was filtered by either sixth-order polynomial (I) or sigmoidal fit (II-III). The sixth-order polynomial was successfully used during the introductory study, but it required further filtering to obtain the acceleration data in a feasible form. The sigmoidal fit was a more optimal choice since it produced a differentiable function. Therefore, the acceleration plot could be directly derived from the velocity plot without further filtering (Fig. 6).

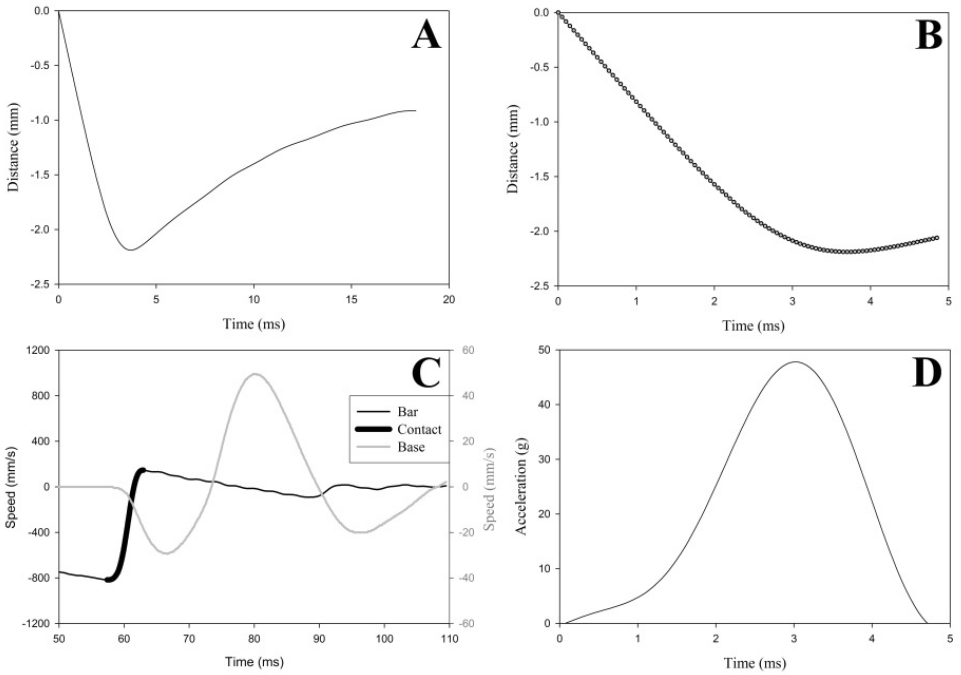

Figure 6. A) Bar displacement near maximum displacement point, B) displacement during contact time, C) velocity graphs and D) acceleration during contact time. (Modified with permission from publication I.)

The displacement plot can be analyzed as is to measure the maximum displacement point and the final displacement level. Force-dependent machine deformation has to be considered to obtain the true maximum displacement point. There is no detectable deformation occurring at the final displacement level as the compression event has already stopped. It is of crucial importance to avoid compression forces high enough to cause permanent deformation in the system.

Since the bar falls in a nearly frictionless manner, the maximum velocity can be roughly estimated from the falling height. For example, a fall from a height of 50 mm results in a velocity of approximately 1000 mm/s. As the vertical speed of the punch during tableting, it can already be considered very high (Konkel & Mielck 1998, Ruegger & Çelick 2000, Zavaliangos et al. 2017). As the bar collides with the punch, the velocity still increases until the acceleration reaches negative values. Therefore, the compressibility of the sample slightly affects the maximum compression speed as well.

The acceleration at collision was calculated by normalizing the values to zero before the collision. This was done to eliminate the numerical value of gravity-based acceleration, which affects both the compressing bar and the sample. In a raw form, the acceleration values are initially negative due to deceleration, but this was changed to absolute values. Therefore, the acceleration begins at zero and ends in zero, as seen in Figure 6. Since the weight of the bar and the surface area of the punch were known, the compression force and pressure could be directly calculated from the acceleration plot. Both maximum pressure and rate of force affect the results during compression, but only the maximum pressure value is considered in this work.

4.2.2.3 Contact time (I-III)

Gravity is the driving force for the falling bar and is only affected by the small amount of friction caused by the bearings. Thus, acceleration remains constant until the bar collides with the punch. Similarly, the acceleration remains constant during springback as the bar is no longer in contact with the punch. Therefore, a section with deviating acceleration can be isolated, and it depicts the time window when the powder compression occurs.

Tableting machines have predetermined movement patterns for the punches and the time of compression is always constant with the settings in use. During G-HVC measurement, the properties of powder dictate the movement pattern. This causes variation in compression pressure and contact times, depending on the sample inside the die. Therefore, instead of being predetermined parameters, pressure and contact time are part of the results obtained from the G-HVC measurement. Falling height affects the pressure and contact time also, as the compression speed increases due to increasing elevation.

Compression speed during G-HVC measurements is generally very high, and the contact times can roughly vary from 2 ms to 15 ms. Short contact times enable the examination of time-dependent viscoelastic phenomena. Had the contact time been longer during the measurements, some of the data may have been lost by favouring plastic behaviour over other compression phenomena. Roughly put, elastic materials generally show longer contact times compared to harder materials, although other factors affect the result as well. In this

work, samples were compressed several times consecutively. Therefore, powder rearrangement was present during the first compression, which generally extended the contact time at that point. During consecutive compressions, the contact time may shorten abruptly after the first compression, which occurs due to compactibility of the material.

4.2.2.4 Machine deformation (I-III)

Machine deformation had to be considered to evaluate the real point of maximum displacement during the compression. This was done by dropping the bar onto an empty die without a sample inside of it. The displacement sensor was set at zero at the bottom of the die and, consequently, negative displacement values were obtained during empty-die-compressions. This was due to machine deformation, and the phenomenon was force-dependent as expected (Fig. 7). Therefore, a correction could be implemented based on the force-deformation plot. During this study, thresholds for permanent deformation were also approximated. It was decided that the falling height limits for 4-mm and 8-mm punches were 7 mm and 40 mm, respectively. These limits ensured that any deformation would recover instantly after compression, which was imperative for the reliability of the results.

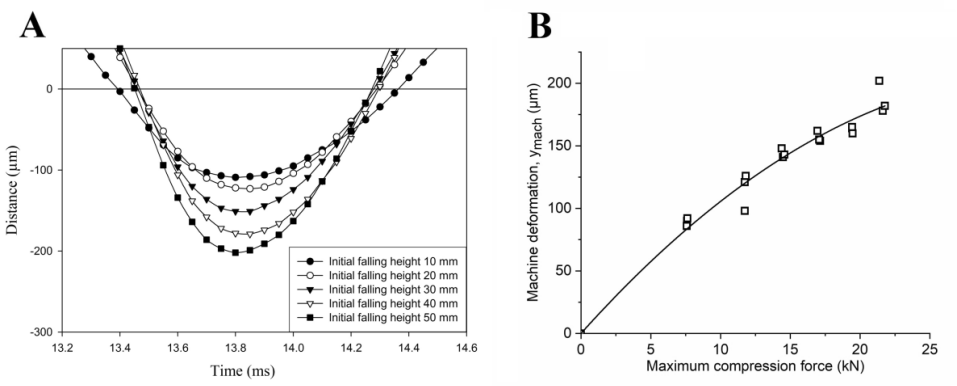

Figure 7. A) Detected machine deformation and B) correlation between maximum compression force and maximum machine deformation. (Modified with permission from publications I and III.)

The amount of maximum machine deformation, y_{mach}, follows the second-order polynomial as:

(10) $$y_{mach}=a \times F + b \times F^2,$$

where F is the maximum compression force. Constants a and b are derived from the fitted plot. Therefore, the true maximum displacement of the bar, y_{maxt}, can be seen as:

(11) $$y_{maxt}=y_{max} + y_{mach},$$

where y_{max} is the detected maximum displacement of the bar.

Determination of the true maximum displacement is crucial to estimate the amount of elastic recovery reliably. Therefore, immediate in-die axial elastic recovery, el_{iia}, can be quantified as:

$$(12) \qquad el_{iia}=100 \text{ x } (y_{final} - y_{maxt})/y_{final},$$

where y_{final} is the final displacement level of the bar.

4.2.2.5 Internal energy change (I-II) and compaction energy calculations (III)

Utilizing G-HVC method, the compaction energy can be estimated in a novel manner. First, an estimation of the internal energy change can be made without a powder sample in the die (Fig. 8). Before falling, the bar has potential energy, which transfers into kinetic energy before collision. When the bar and punch collide without powder in the die, energy is mainly transferred into heat, vibrations, the kinetic energy of surroundings and sound. These can be considered machine-originated factors of energy loss during the collision. Due to energy loss, the springback height of the bar is not as high as the original position. Thus, the internal energy change, ΔE, after the first impact equals the difference between these two values of potential energy.

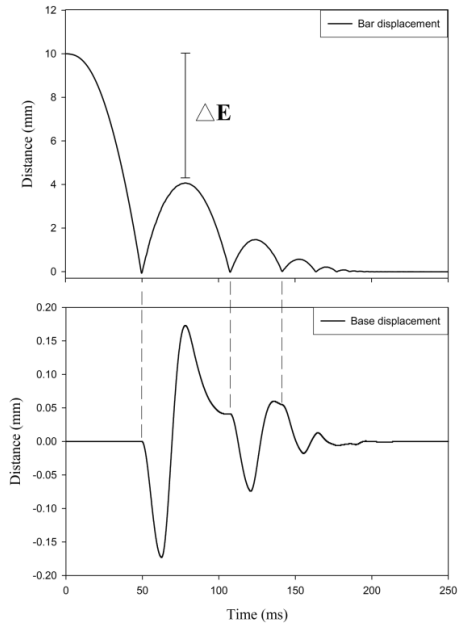

Figure 8. Bar and base displacement during measurement without powder. ΔE is internal energy change. (Reprinted with permission from publication I.)

When powder sample is applied inside the die, some of the energy loss occurs due to compact formation. Estimating the compaction energy can be complicated since the total energy consumption is divided into machine-originated and sample-originated factors. However, an estimation of the machine-originated factors can be done by monitoring the base displacement, as seen in Figure 8. When there is no powder inside the die, the base movement corresponds to the springback height of the bar, serving as an indicator for the machine-originated energy loss. Instead of the maximum displacement of the base, the maximum velocity value is used to avoid facing a displacement limit in the deformation (Fig. 9). This could be compared to compressing a spring between your fingers. There is a limit for the displacement of the spring, but there is no limit on how quickly this limit can be reached.

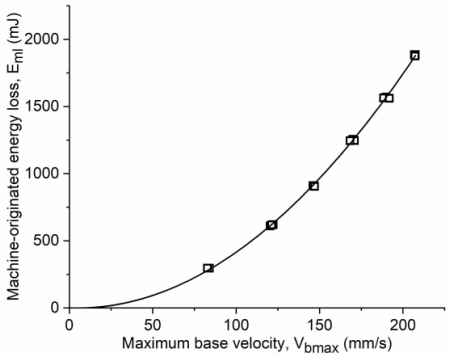

Figure 9. Machine-originated energy loss. (Reprinted with permission from publication III.)

When the powder is applied in the die, the base displacement is used as an indicator for machine-originated energy loss. There is an assumption that the amount of energy not transferred into the compact is always causing similar deformation in the base. This contains some errors as some phenomena, such as heat formation, occur differently whether there is powder present or not. For this study, this calculation method was considered to be the best estimation for machine-originated energy loss. Force-displacement plot is often used for compaction energy estimations. Without any corrections, all these error factors are present in the area under the force-displacement curve.

After consecutive compressions, samples eventually reach a state where no more permanent deformation can be seen. In other words, the yield pressure of the sample increases by each compression. Therefore, each sample should show zero internal energy change when the yield pressure exceeds the applied pressure. It was noticed, however, that there was still detectable residual internal energy change present. This was notably relatable to the elastic recovery of the sample. It was assumed that the residual energy occurs due to energy transferring into temporary elastic potential during compression. This phenomenon would not contribute to the springback height of the bar and, therefore, remained undetectable. This sample-originated factor was assumed as a constant to be considered at each compression of a set.

With all these factors considered, an estimation of compaction energy could be made as:

(13) $E_{tot} = M \times g \times (y_{init} - y_{maxt})$,

where E_{tot} is the total potential energy input in the system, g is gravitational acceleration, M is the weight of the bar, and y_{init} is the original falling height of the bar.

The amount of total non-elastic energy, E_{ne}, can be seen as:

(14) $E_{ne}=E_{tot} - (M \times g \times y_{reb})$,

where y_{reb} is the highest rebound height during springback of the bar. Friction between the bar and bearings can be ignored at this point since its contribution is included in the rebound height.

Machine-originated energy loss, E_{ml}, is related to the maximum base velocity, V_{bmax}, and can be stated in the second-order form:

(15) $E_{ml}=c \times V_{bmax} + d \times V_{bmax}^2$,

where c and d are constants defined from the compressions without powder in the die.

The amount of energy consumed in immediate elastic recovery, E_{rec}, can be seen as:

(16) $E_{rec}=M \times g \times (y_{final} - y_{maxt})$

The sample-originated energy loss, E_{sl}, is defined from the fifth compression of each set as:

(17) $E_{sl}=E_{ne5} - E_{ml5} - E_{rec5}$,

where E_{ne5} is the total non-elastic energy during the fifth compression, E_{ml5} is the machine-originated energy loss during the fifth compression, and E_{rec5} is the recovered elastic energy at fifth compression. It is assumed that during the fifth compression of a set, yield pressure of the sample exceeds the applied pressure.

Compaction energy, E_{comp}, can be then estimated as:

(18) $E_{comp}=E_{ne} - E_{rec} - E_{ml} - E_{sl}$

Consequently, the compaction energy at the end of each set, E_{comp5}, always equals zero:

(19) $E_{comp5}=E_{ne5} - E_{rec5} - E_{ml5} - E_{sl}$

(20) $E_{comp5} = E_{sl} - E_{sl} = 0$

Specific compaction energy, E_{comps}, can be stated as:

(21) $E_{comps}=E_{comp}/w_s$,

where w_s is sample weight.

4.2.3 Fluid bed granulation, particle size analysis and tableting (III)

Fluidized bed granulator (Glatt WSG 5, Glatt GmbH, Binzen, Germany) was used to produce granules from three different formulations (Table 1). HPMC was added to the powder formulations, and water was used as a granulation liquid. Finally, granules were forced through a 1000 µm sieve. In-line particle probe (Parsum IPP 70-SE, Parsum GmbH, Chemnitz, Germany) was used to measure the particle size distribution of the granules.

Table 1. Powder mixtures (PM=physical mixture and FBG=fluid bed granules).

	Weight-%				
	MCC	**DCP**	**HPMC**	**Theophylline**	**Magnesium stearate**
Formulation 1: PM1/FBG1	73	20	5	1	1
Formulation 2: PM2/FBG2	68	20	10	1	1
Formulation 3: PM3/FBG3	58	20	20	1	1

An instrumented eccentric, single-station tableting machine (Korsch EK 0, Erweka GmbH, Heusenstamm, Germany) was used to produce tablets from fluid bed granules. A round and flat-faced punch with a diameter of 9 mm was in use. Three different granule batches were compacted with three different force levels, producing nine different tablet batches. For each tablet batch, one hundred tablets were collected. Transparent plastic tubes were used to collect the tablets in order. Thus, properties of each tablet could be compared to the corresponding compression event, in terms of upper punch pressure. Twenty tablets were picked from each batch, equalling 180 tablets in total. Dimensions of these tablets were measured with a digital micrometer (Sony DZ521, Tokyo, Japan). Hardness tester (Schleuniger 2E, Dr Schleuniger Pharmatron AG, Solothurn, Switzerland) was used to measure crushing strength for these tablets. Tensile strength was calculated utilizing Equation 8.

4.2.4 Other powder sample analysis and preparation methods (I-III)

Before compressions, all powder samples were individually weighed by an analytical balance. Water activity meter (AquaLab Series 3, Decagon Devices Inc., Pullman, Washington, USA) was used to measure the water activity of the samples. Room temperature and relative humidity were monitored with a moisture tester (Mastech MS6900, Precision Mastech, City of Industry, California, USA). A helium pycnometer (Multivolume Pycnometer 1305, Micromeritics Inst. Corp., Norcross, GA, USA) was used to measure the true density of the samples (II-III). Multiple consecutive measurements were made to aid the removal of any residual water in the samples. Some of the samples were also dried in an oven (II). Specific temperatures and heating times were used to avoid melting and polymorphism.

5 Results and discussion

5.1 Observing particle deformation and compact formation (I-III)

5.1.1 Elastic recovery (I-III)

The difference between the maximum and final displacement levels depicts the immediate in-die axial elastic recovery, el_{iia}. It is crucial to note that the material would often recover more after ejecting out of the die (I). Therefore, results from different studies in the field must be compared with the precise knowledge of each method in use.

When compressing samples five times consecutively, the elastic recovery did not tend to change remarkably between compressions. Typically, it increased slightly during the later compressions. This was assumed to be due to an increase in compression pressure and a decrease in the contact time during the collision. This is explained by the hardening of the sample during consecutive compressions. During later compressions, the pressure did not exceed the yield pressure to consolidate the sample remarkably further, and only elastic deformation occurred at that point. Therefore, the elastic recovery values were collected from the fifth compression of each set.

The approximate elastic recovery values obtained throughout the study have been compiled in Figure 10. Starches and HPMC appeared to be the most elastic of all the materials. Fragmenting materials and theophylline showed lower values of elastic recovery, and MCC was set in between. The results were in agreement with the existing literature (Bassam et al. 1990, Van Der Voort Maarschalk et al. 1997, Picker 2001, Hardy et al. 2006, Anuar & Briscoe 2009, Chattoraj et al. 2010, Haware et al. 2010, Mazel et al. 2013, Chang & Sun 2017).

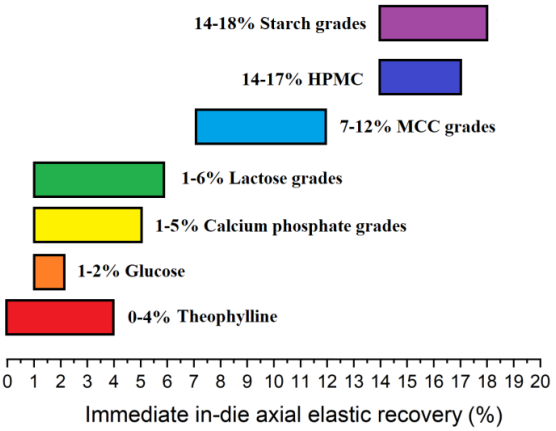

Figure 10. Approximate elastic recovery values of studied materials (I-III).

Even though the hardness of the compacts formed after G-HVC compressions was not specifically studied, it was noted that starches produced very weak compacts which could easily break during and after ejection. It is important to note that G-HVC method allows the examination of mechanical properties even when no coherent compact is necessarily formed. Similar breakage was not observed in HPMC compacts even though the amount of elastic recovery was roughly the same. This served as a fine example that not only the mechanical properties necessarily dictate the outcome. HPMC is used as a binder often mixed in a liquid, but it also acts as an excellent dry binder (Kolter & Flick 2000). Supposedly, HPMC particles had more bonding potential with each other when compared to starch particles. It is also important to remember that in actual tableting formulations, having only one material in a formulation is quite rare. Thus, the presence of different ingredients in a mixture can drastically change or simply overcome the expected behaviour of any individual material.

When different physical formulations (PM1-PM3) and corresponding fluid bed granules (FBG1-FBG3) were studied, the overall elastic recovery remained at an expected level when compared to results from the individual ingredients (III). However, no significant difference in elastic recovery was noted between them. This was slightly unexpected since the amount of elastic HPMC was notably higher in some of the formulations. This could mean that the dominant excipient in the mixture, MCC, could entrap the elastic materials inside the overall structure. This assumption could be related to percolation theory. Abrupt changes in tabletability may be observed as certain thresholds have been exceeded in relative portions of materials in a formulation. Consequently, the elastic stress may have remained in the compact even after ejection. One could assume that at least two possible outcomes exist in this situation. The stress relaxation could occur over time, in which case the tablet would remain intact. However, the tablet could rupture if the elastic relaxation did not occur, and the elastic stress would overcome the cohesive forces in the compact. Without a specific study, the unwanted outcome cannot be seen until after it has happened during storage. Therefore, any “hidden” elasticity in a mixture could be seen as a warning sign when designing a durable tablet formulation.

5.1.2 Relative volume reduction (I)

When compressing materials consecutively five times, the progression of maximum and final displacement levels can be observed directly to evaluate deformation behaviour. In Figure 11, MCC (Avicel PH-102) and starch (Amioca TF) showed dissimilar consolidation in terms of relative volume change (I). The volume at point one refers to the bulk in-die-volume of the sample, which can be calculated directly from the powder bed height. It can be observed that MCC can be compacted into less than half of its original volume, whereas starch resists further change under 60-70% relative volume. Out of these two materials, starch showed generally lower compressibility and higher elastic recovery. Both materials seemed to undergo volume decrease gradually by each compression, and this can be an indicator of plastic behaviour. Fragmenting materials could show abrupt and rapid volume decrease, as long as the compression pressure would exceed the required yield point.

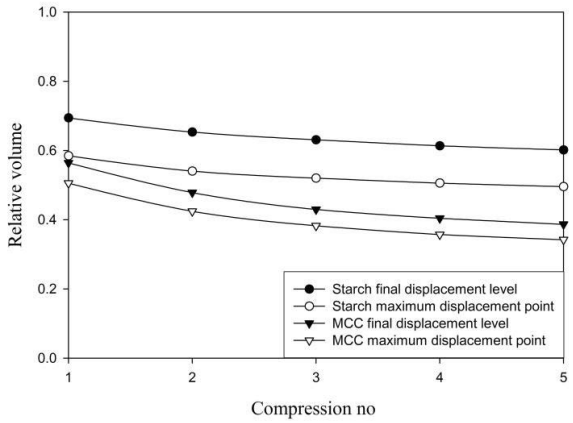

Figure 11. Relative volume reduction after five compressions of starch (Amioca) and MCC (Avicel PH-102). (Reprinted with permission from publication I.)

It is of importance to understand that the relative volume change alone does not depict the ability of the material to produce a decent compact. Remarkable volume change and minimal elastic recovery may serve as initial marker flags for good compactibility, as long as this knowledge is interpreted with caution.

5.1.3 Porosity change (II)

Increase in solid fraction of the sample generally leads to harder compacts (Tye et al. 2005, Reynolds et al. 2017). However, the exact hardness of the compact is always dependent on the properties of the starting materials. For example, tablets made of dry-granulated material may show high solid fraction but poor tabletability.

Porosity change can be examined similarly to relative volume change with the G-HVC method. The true density of the material has to be measured to evaluate the porosity of the material. If a material can be compacted into its true density point, the solid fraction value is considered 100% and porosity value 0%. In other words, porosity refers to the amount of air in the compact.

Examination of porosity change can be utilized to evaluate the ability of the material to reach its true density. The porosity change at the final displacement level for eight different materials is shown in Figure 12. Inclusion of porosity at maximum displacement point would also allow the observation of elastic recovery, similarly to the relative volume plot. Two different setups were in use, where *Setup A* had higher compression pressure and lower compression speed than *Setup B*. Consequently, *Setup A* would generally show enhanced compressibility when compared to *Setup B*.

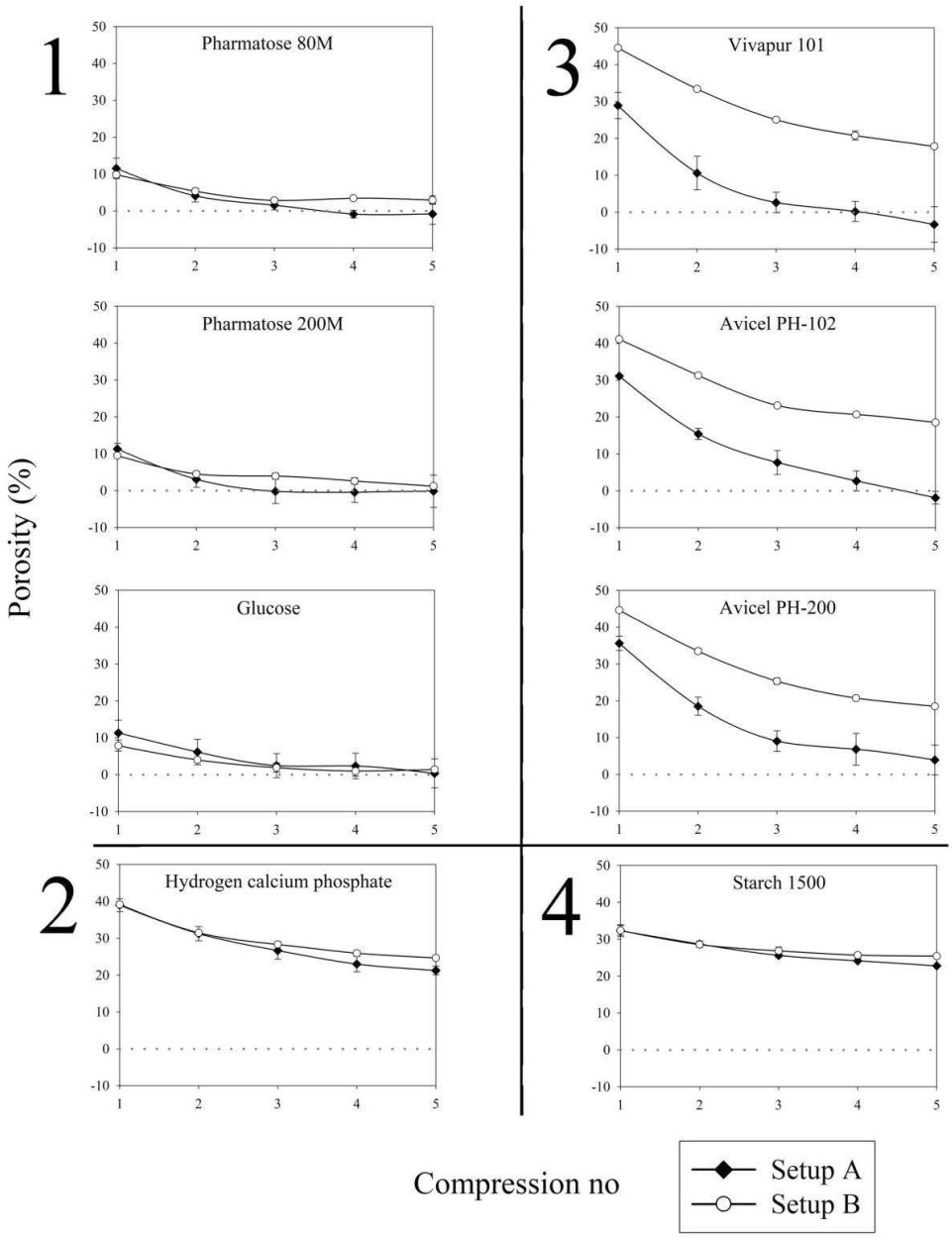

Figure 12. In-die porosity after five consecutive compressions. 1) Fragmenting materials (fracture pressure exceeded), 2) fragmenting material (fracture pressure not exceeded), 3) plastic materials and 4) elastic material. (Reprinted with permission from publication II.)

Two grades of lactose and glucose were categorized as fragmenting materials with a lower fracture point than the compression pressure (Fig. 12-1). All three materials showed

remarkable compressibility during first two compressions, and only minimal consolidation was observed during the last three compressions. All three materials seemed to reach the true density, and the results were independent of the setup in use. These materials also showed minimal elasticity (Fig. 10).

Different grades of MCC were significantly more dependent on the setup in use (Fig. 12-3). Higher pressure setup had a remarkable impact on the samples, some of which even reached the true density value. The shapes of the curves are similar, though, indicating a gradual decrease of porosity by each compression. These were seen as indicators for plastic behaviour. Plasticity occurs in a time-dependent manner, and G-HVC method typically produces high compression speed. Had the compression speed been lower and contact time longer, the curves could have been near straight lines similar to fragmenting materials in Figure 12-1.

Calcium hydrogen phosphate (Fig. 12-2) and Starch 1500 (Fig. 12-4) produced quite similar graphs, while their mechanical properties are very different from each other. However, starch is immensely more elastic than calcium phosphate and shows more steady decrease in porosity. Calcium phosphate is a fragmenting material with a high yield pressure point, which was not exceeded in this work. Consequently, it was impossible to reach the true density in this case. Using a compression pressure higher than the yield point resulted in permanent deformation of the punch, which then had to be replaced. Had there been more different setups in use, the pressure dependency for starch could have been more visible. At low-pressure levels, the graphs may have resembled those of MCC (Fig. 12-3). Scanning electron microscopy could also be used to confirm the presence of partially fragmented calcium phosphate particles at a shear surface.

In conclusion, all eight materials could be differentiated in terms of their mechanical properties utilizing the G-HVC method. This study also proved to be a good example of having to exercise caution when interpreting results from only one angle. Had one only examined the porosity decrease at the final displacement level, one could have incorrectly categorized starch and calcium phosphate as similar in terms of mechanical properties.

5.2 Comparison of G-HVC-based compaction energy estimation and tableting (III)

5.2.1 Tensile strength of the tablets

Tablets were compacted from fluid bed granules (FBG1-FBG3) with three different force levels. Since the tablets were collected in tubes in order, each one could be compared to the upper punch pressure value from the corresponding compaction event (Fig. 13). Tablets prepared from FBG1 and FBG2 were very similar in terms of tensile strength. Tablets compacted from FBG3 had significantly lower tensile strength. This was due to the lower content of MCC and higher content of HPMC in FBG3. MCC was the dominant ingredient in the mixtures, and it would seem that a percolation threshold existed between FBG3 and

the rest of the formulations. Even if the settings in the eccentric machine were kept constant, there was a slight variation in compaction pressure levels. This was probably due to differences in formulations. One could assume that FBG3 resisted deformation more than the rest of the mixtures, and more pressure was required to compress the samples into the desired volume. There was no remarkable variation in tablet weights, which served as a proof of uniform die filling.

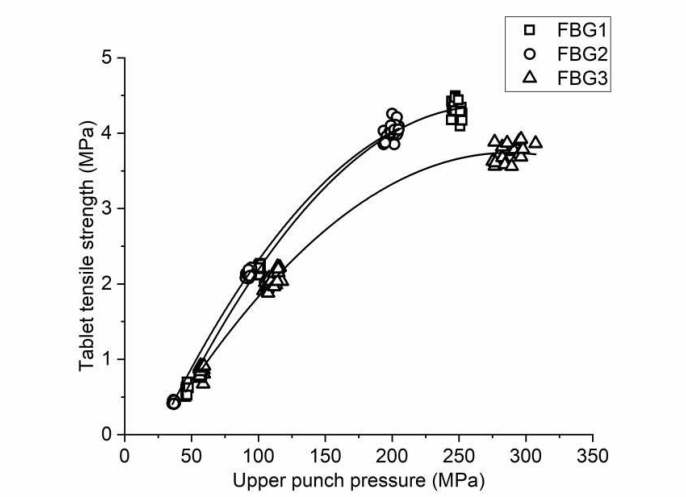

Figure 13. The correlation between the upper punch pressure and tablet tensile strength with three different force levels. (Reprinted with permission from publication III.)

5.2.2 Compaction energy determined by G-HVC method

Specific compaction energy for individual ingredients included in the formulations can be seen in Figure 14. The fifth compression was omitted due to the assumption that no more consolidation was occurring at that time. Magnesium stearate was considered to serve as an obligatory lubricant and was not explicitly studied in this work. In short, high amounts of magnesium stearate significantly impairs the tabletability of the mixture (Aoshima et al. 2005, Late et al. 2009, Koskela et al. 2018). In this study, the amount of magnesium stearate in the formulations was reasonable.

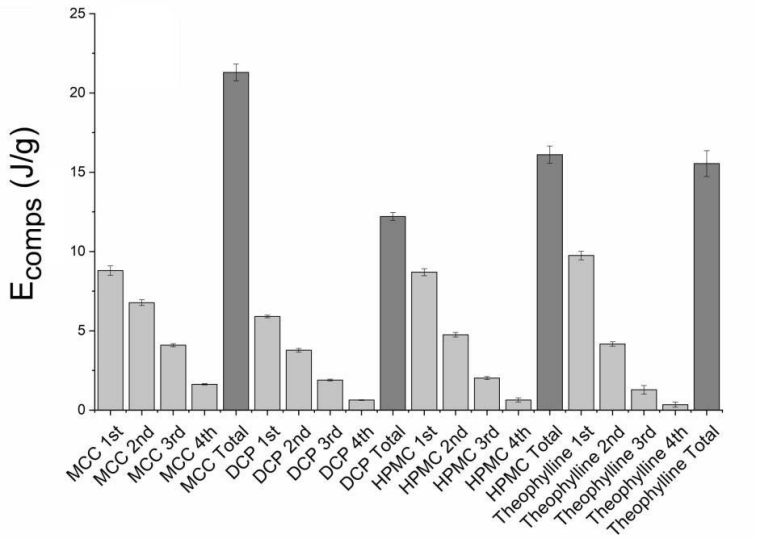

Figure 14. Specific compaction energy for individual mixture ingredients. (Reprinted with permission from publication III.)

In total, the largest amount of compaction energy was bound in MCC, followed by HPMC, theophylline and finally DCP (Fig. 14). To ensure roughly similar energy input onto all of the samples, the sample weights varied due to differences in material density. The sample weight was decided so that the final displacement level would be at 1 mm, should the sample reach its true density. The sample weight for DCP was higher, which lowers the specific compaction energy value. On the other hand, HPMC was lighter, which resulted in lower sample weight and higher specific compaction energy value. Therefore, comparing individual ingredients in this manner only can be problematic. For this study, it was decided that the uniform energy input was more important. Also, in the study of mixtures, the weight was similar for all samples.

The graph shown in Figure 14 may aid in evaluating the loss of tabletability due to precompression. The compaction energy after the first compression and the subsequent compressions can be compared to see the decline in energy bind. MCC shows a very steady decrease of compaction energy in consecutive compressions and less than half of the total energy is bound during the first compression. On the other end of the graph, it can be seen that a substantial amount out of total energy is bound in theophylline during the first compression. It is widely known that plastically deforming theophylline shows excellent compressibility. However, based on this result, theophylline could be susceptible to the loss of tabletability when precompression is required. The bonding potential could be lost during dry granulation, for example, where the mixture is compacted into ribbons before milling them to granules. The particle size increase of dry granules has also been suggested as a possible cause for the loss of tabletability. It is important to remember, that among various studies, there may be differences in contact time or compaction pressure during precompression phase and actual tablet compaction phase, which affect the results. For example, Hadžović et al. (2011) reported that the decrease of compactibility was more

apparent for MCC than theophylline. Herting and Kleinebudde (2007) observed an overall loss of tabletability in binary mixtures consisting of MCC and theophylline. Sun and Himmelspach (2006) also noticed that the tensile strength of the MCC tablets decreased due to dry granulation. In this work, a more comprehensive study would be required to confirm the magnitude of the loss of tabletability. In this study, however, a direct comparison of MCC and theophylline would nevertheless suggest that, out of the two, MCC could be more suitable for multiple compressions.

When comparing mixtures, fluid bed granules showed clearly more energy intake than their corresponding physical mixtures (Fig. 15). The results are in agreement with existing literature as fluid bed granulation has been reported to enhance the tabletability of the powder (Li & Peck 1990, Arndt et al. 2018). Formulation 3 showed generally lower energy intake than the rest of the batches.

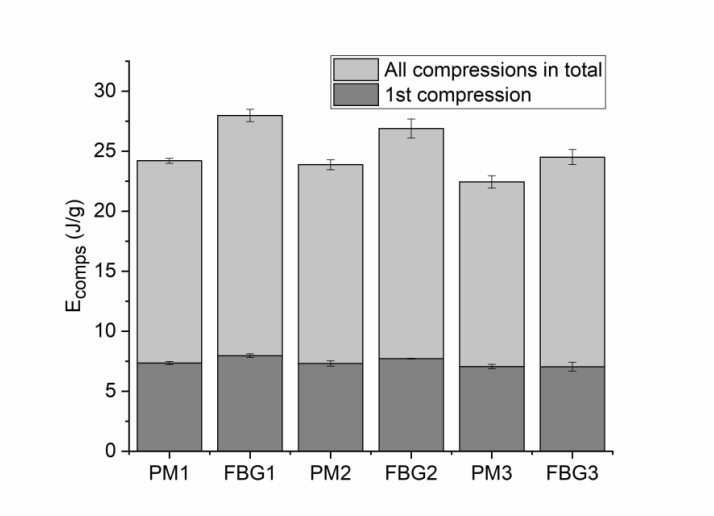

Figure 15. Specific compaction energy for mixtures. (Reprinted with permission from publication III.)

5.2.3 Modelling compaction energy vs. tablet tensile strength

Tensile strength of all the tablets could be compared without extrapolation between 100 and 200 MPa punch pressure (Fig. 13). Therefore, these two values were selected for the compaction energy-tensile strength model. Due to differences in sample properties, the compression pressure varied slightly during G-HVC measurements. Therefore, the lowest pressure value obtained during a set of repetitions was set at 100 or 200 MPa, and the rest of the samples were modelled by a relative increase in pressure. Thus, the expected increase in tensile strength due to pressure increase had been considered individually for each sample. Only the first compression of each set was deemed to be relevant for the model.

Both models showed a good correlation between compaction energy determined by G-HVC method and the tensile strength of tablets compacted with a tableting machine (Fig. 16). The model set at 200 MPa pressure (Fig. 16-B) seemed to be more reliable than the one set at 100 MPa (Fig. 16-A). This could be a direct consequence due to more apparent differences in tensile strength with higher pressure (Fig. 13). There were no significant differences between FBG1 and FBG2, which was to be expected from the other results of this work. However, one could have correctly discarded FBG3 by the results from G-HVC calculations alone, had the aim been to produce harder tablets. Therefore, it was proven that the G-HVC method produced relevant results that could be utilized in practice.

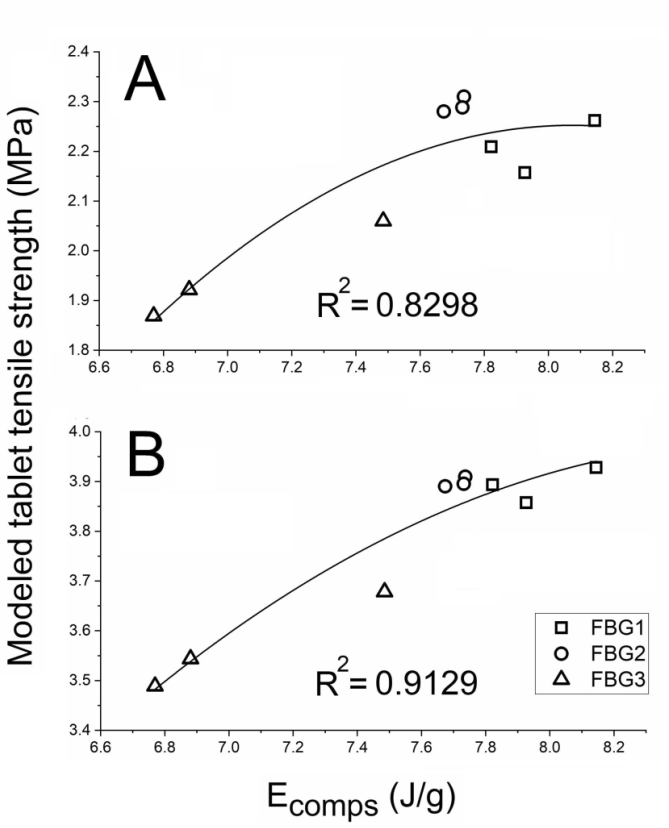

Figure 16. Correlation between the specific compaction energy of the first compression of each set obtained from G-HVC measurements and the tablet tensile strength obtained from the tableting machine. Model pressure values were A) 100 MPa and B) 200 MPa. (Reprinted with permission from publication III.)

5.3 Other general discussion and future studies

G-HVC method was not created as an alternative to more comprehensive tableting simulators but to act as a simple, small and cost-efficient tool for very early stages of pharmaceutical product development. The experiments conducted utilizing the G-HVC method could be applicable before proceeding to studies with a more complex tableting simulator. New APIs are often available in small amounts, so being able to study new materials with small sample sizes is also beneficial. Regardless of the settings in use, the compression speed is always high, and the contact time during compression is often under ten milliseconds. Studying mechanical properties with high speed is comparable to modern tableting machines with remarkably high tablet output. However, it is good to remember, that longer contact times during actual tableting can lead to decent compacts, even though G-HVC results would initially suggest otherwise. Therefore, it is essential to see the whole picture when doing tableting simulations.

In the future, more materials and their polymorphs could still be studied with the method to form a more coherent understanding of compression behaviour. It can also be assumed that the G-HVC displacement data has more potential than the present studies show. By observing the descending part of the displacement curve, one could obtain information regarding the rearrangement of particles. The height of compression could also be set so low, that only rearrangement would occur. The impact of different particle sizes could also be studied this way. Being able to quantify the effect of die-wall forces by this manner could not be ruled out either.

Compaction energy could also be observed from another angle. By varying the falling height and compression force, not only the specific but also the relative amount of compaction energy could be studied. During G-HVC studies, the compaction energy was never 100% of the total energy input. However, for some materials, such as MCC, it was not that far off either. It would be interesting to see if some of the materials would always resist deformation or show good compactibility regardless of the magnitude of the energy input. By this manner, an attempt could be made to create a classification system based on the energy binding potential of each material which could be depicted by relative compaction energy range instead of specific values.

Rate of force was not studied comprehensively, and maximum force values were used instead throughout the study. This produces some error since the rate of force and AUC of the force-time curve (depicting impulse) affect the estimations of machine deformation. In future studies, the rate of force could be included in the estimations.

The method is unique in a way that the properties of the powder sample ultimately define the displacement pattern of the falling bar. The sensitiveness of the method allows accurate examination of any material providing undistorted information. This also means that any predetermined parameter, other than the total energy input, is difficult to adjust. The collision is more abrupt for less elastic materials due to shorter contact time. For these materials, a lower falling height would need to be set to cause a similar maximum compression pressure compared to more elastic materials. In that case, the total energy input and compression speed would change as well. An adjustable weight could be implemented for a future model of the device, which could allow keeping the compression speed constant.

Another way to improve the adjustability of the method could be the use of any fixed acceleration besides gravity. This modification could be carried out by utilizing counterweight or friction, to suggest a few possible solutions. The basic principle would be the same, and the displacement pattern would still be only dependent on the properties of the powder. This modification could allow remarkable flexibility in terms of compression pressure and speed. Therefore, acceleration adjustment is something to consider when designing further studies.

While the device used in the studies is remarkably smaller than a tableting machine, it could still be further miniaturized. Since the compaction energy calculus was proven to be quite reliable, a study could also be carried out with a “tabletop”-model to see if the tensile strength model would still be applicable. This could allow the use of even smaller sample sizes than the ones used in this work. However, new challenges would arise as the impact of die-wall forces could turn out to be remarkable when using dies with a small diameter. Also, the inclusion of larger particles could easily distort the results. At best, the smaller device could function quite similarly in terms of compaction energy estimation. This enhancement will be considered for further studies.

So far, the compaction energy-tensile strength comparison is the only G-HVC study conducted with actual tableting involved. Even if the method was not used as a tableting simulator per se, it could provide helpful information about mechanical properties for any individual material or mixture. In summary, it could be stated that utilizing the G-HVC method makes one wiser about the materials one is working on. Residual elastic stress in mixtures or indicators for loss of tabletability could be initially marked as red flags even though these phenomena would not always end up causing any defects.

6 Conclusions

In this thesis, the applicability of the G-HVC method was evaluated as a novel tool to study the mechanical properties of pharmaceutical powders. Powder deformation phenomena and estimation of tabletability were studied with the method. Both individual ingredients and actual tablet formulations were studied.

First, introductory studies were carried out to determine various factors concerning the method. Machine deformation was detected, and a force-dependent correlation was produced to evaluate its magnitude. Displacement data could be directly studied from the data. A novel computer program was coded to derive velocity and acceleration from these displacement graphs. Internal energy change was evaluated based on the springback of the bar and the deformation wave in the base. During the introductory studies, it was shown that starch and MCC behaved differently. Starch showed more elasticity and was less compressible than MCC. It was demonstrated that the method was functional and provided results that were in agreement with the existing knowledge of the studied materials.

During the second study, eight different materials were studied with two different energy input levels causing variation in compression pressure. Lactose grades and glucose showed little elasticity and seemed to fragment well as the samples reached true density with both setups. The compression pressure was not sufficient to exceed the high yield pressure of fragmenting anhydrous calcium phosphate. MCC grades showed plastic deformation and were the most pressure-dependent of all the studied materials. Starch was the most elastic of all samples. It was concluded that the method showed a clear difference between the studied materials and, based on the results, compaction behaviour for each material could be estimated.

In the third study, formulations consisting of MCC, calcium phosphate, theophylline and HPMC were examined. Materials were also studied individually. Three different formulations were granulated using a fluid bed system, and tablets were compacted from the granules. The loss of tabletability due to precompression was seen as a possible outcome for some materials, such as theophylline, which lost their bonding potential quickly during consecutive compressions. It was noted that formulations with a higher content of elastic HPMC did not show higher elastic recovery. It was discussed that the dominant MCC might have encapsulated HPMC in the overall structure, possibly leading to residual elastic stress. This elastic potential could then fracture the compact over time if stress relaxation did not occur. Both machine-originated and sample-originated factors were further considered to polish the energy calculations to approximate the compaction energy more reliably. The compaction energy values determined with the G-HVC method showed a good correlation with the tensile strength of the tablets prepared with a tableting machine. One could have correctly discarded the weakest formulation based on G-HVC results alone, had the aim been to produce tablets with higher tensile strength. Therefore, it was shown that a practical estimation of tabletability of the mixtures could be done utilizing the method.

In conclusion, the G-HVC method was proven to be a simple, cost-efficient and reliable tool in the examination of mechanical properties of various powders and powder mixtures. It was shown that relevant information regarding powder compression and compaction could be obtained by simply dropping a weight on a powder sample while monitoring its

displacement. The numerical results were in agreement with the existing literature. The estimation of tabletability showed that the method could be of practical use. The G-HVC method fits well in the early phases of modern pharmaceutical tablet development, where novel material-sparing, cost-efficient and reliable methods are always in demand.

References

Abdel-Hamid S., Alshihabi F. & Betz G. Investigating the effect of particle size and shape on high speed tableting through radial die-wall pressure monitoring. Int. J. Pharm. 413, 29–35, 2011.

Abrantes C. G., Duarte D. & Reis C. P. An Overview of Pharmaceutical Excipients: Safe or Not Safe? J. Pharm. Sci. 105, 2019–2026, 2016.

Aburub A., Mishra D. & Buckner I. Use of compaction energetics for understanding particle deformation mechanism. Pharm. Dev. Technol. 12, 405–414, 2007.

Adolfsson Å. & Nyström C. Tablet strength, porosity, elasticity and solid state structure of tablets compressed at high loads. Int. J. Pharm. 132, 95–106, 1996.

Akande O. F., Ford J. L., Rowe P. H. & Rubinstein M. H. The effects of lag-time and dwell-time on the compaction properties of 1:1 paracetamol/microcrystalline cellulose tablets prepared by pre-compression and main compression. J. Pharm. Pharmacol. 50, 19–28, 1998.

Akseli I., Ladyzhynsky N., Katz J. & He X. Development of predictive tools to assess capping tendency of tablet formulations. Powder Technol. 236, 139–148.

Allam A. N., El Gamal S. S. & Naggar V. F. Bioavailability: a pharmaceutical review. J. Novel Drug Deliv. Tech. 1, 77–93, 2011.

Alonzo D. E., Zhang G. G. Z., Zhou D., Gao Y. & Taylor L. S. Understanding the behavior of amorphous pharmaceutical systems during dissolution. Pharm. Res. 27, 608–618.

Amin M. C. I. & Fell J. T. Comparison studies on the percolation thresholds of binary mixture tablets containing excipients of plastic/brittle and plastic/plastic deformation properties. Drug Dev. Ind. Pharm. 30, 937–945, 2004.

Anbalagan P., Liew C. V. & Heng P. W. S. Role of dwell on compact deformation during tableting: an overview. J. Pharm. Investig. 47, 173–181, 2017.

Antikainen O. & Yliruusi J. Determining the compression behaviour of pharmaceutical powders from the force–distance compression profile. Int. J. Pharm. 252, 253–261, 2003.

Anuar M. S. & Briscoe B. J. The elastic relaxation of starch tablets during ejection. Powder Technol. 195, 96–104, 2009.

Aoshima H., Miyagisnima A., Nozawa Y., Sadzuka Y. & Sonobe T. Glycerin fatty acid esters as a new lubricant of tablets. Int. J. Pharm. 293, 25–34, 2005.

Arndt O.-R., Baggio R., Adam A. K., Harting J., Franceschinis E. & Kleinebudde P. Impact of different dry and wet granulation techniques on granule and tablet properties: a comparative study. J. Pharm. Sci. 107, 3143–3152, 2018.

Ayorinde J. O., Itiola O. A. & Odeniyi M. A. Effects of material properties and speed of compression on microbial survival and tensile strength in diclofenac tablet formulations. Arch. Pharm. Res. 36, 273–281, 2013.

Bacher C., Olsen P. M., Bertelsen P. & Sonnergaard J. M. Compressibility and compactibility of granules produced by wet and dry granulation. Int. J. Pharm. 358, 69–74, 2008.

Badawy S. I. F., Gray D. B. & Hussain M. A. A Study on the Effect of Wet Granulation on Microcrystalline Cellulose Particle Structure and Performance Pharm. Res. 23, 634–640, 2006.

Baronsky-Probst J., Möltgen C.-V. Kessler W. & Kessler R. W. Process design and control of a twin screw hot melt extrusion for continuous pharmaceutical tamper-resistant tablet production. Eur. J. Pharm. Sci. 87, 14–21, 2016.

Bassam F., York P., Rowe R. C. & Roberts R. J. Young's modulus of powders used as pharmaceutical excipients. Int. J. Pharm. 64, 55–60, 1990.

Bateman S. D., Rubinstein M. H., Rowe R. C. Roberts R. J., Drew P. & Ho A. Y. K. A comparative investigation of compression simulators. Int. J. Pharm. 49, 209–212, 1989.

Berggren J., Frenning G. & Alderborn G. Compression behaviour and tablet-forming ability of spray-dried amorphous composite particles. Eur. J. Pharm. Sci. 22, 191–200, 2004.

Blessy M., Patel R. D., Prajapati P. N. & Agrawal Y. K. Development of forced degradation and stability indicating studies of drugs—A review. J. Pharm. Anal. 4, 159–165, 2014.

Bolhuis G. K. & Armstrong N. A. Excipients for direct compaction—an update. Pharm. Dev. Technol. 11, 111–124, 2006.

Buckner I., Friedman R. A. & Wurster D. E. Using compression calorimetry to characterize powder compaction behavior of pharmaceutical materials. J. Pharm. Sci. 99, 861–870, 2010 (a).

Buckner I. S., Wurster, D. E. & Aburub A. Interpreting deformation behavior in pharmaceutical materials using multiple consolidation models and compaction energetics. Pharm. Dev. Technol. 15, 492–499, 2010 (b).

Busignies V., Leclerc B., Porion P., Evesque P., Couarraze G. & Tchoreloff P. Compaction behaviour and new predictive approach to the compressibility of binary mixtures of pharmaceutical excipients. Eur. J. Pharm. Biopharm. 64, 66–74, 2006.

Cantor S. L., Kothari S. & Koo O. M. Y. Evaluation of the physical and mechanical properties of high drug load formulations: Wet granulation vs. novel foam granulation. Powder Technol. 195, 15–24, 2009.

Casas M., Galdón E., Ojeda D. J. & Caraballo I. Thermoplastic polyurethane as matrix forming excipient using direct and ultrasound-assisted compression. Eur. J. Pharm. Sci. 136, 104949, 2019.

Cascone S., De Santis F., Lamberti G. & Titomanlio G. The influence of dissolution conditions on the drug ADME phenomena. Eur. J. Pharm. Biopharm. 79, 382–391, 2011.

Çelik M. Overview of compaction data analysis techniques. Drug Dev. Ind. Pharm. 18, 767–810, 1992.

Chang S.-Y. & Sun C. C. Superior plasticity and tabletability of theophylline monohydrate. Mol. Pharm. 14, 2047–2055, 2017.

Charlton B. & Newton J. M. Theoretical estimation of punch velocities and displacements of single-punch and rotary tablet machines. J. Pharm. Pharmacol. 36, 645–651, 1984.

Chattoraj S., Shi L. & Sun C. C. Understanding the relationship between crystal structure, plasticity and compaction behaviour of theophylline, methyl gallate, and their 1:1 co-crystal. CrystEngComm. 12, 2466–2472, 2010.

Chieng N., Rades T. & Aaltonen J. An overview of recent studies on the analysis of pharmaceutical polymorphs. J. Pharm. Biomed. Anal. 55, 618–644, 2011.

Cleveringa H. H. M., Van der Giessen E. & Needleman A. A discrete dislocation analysis of mode I crack growth. J. Mech. Phys. Solid. 48, 1133–1157, 2000.

Coffin-Beach D. P. & Hollenbeck R. G. Determination of the energy of tablet formation during compression of selected pharmaceutical powders. Int. J. Pharm. 17, 313–324, 1983.

Csóka I., Pallagi E. & Paál T. L. Extension of quality-by-design concept to the early development phase of pharmaceutical R&D processes. Drug Discov. Today 23, 1340–1343, 2018.

DeCrosta M. T., Schwartz J. B., Wigent R. J. & Marshall K. Thermodynamic analysis of compact formation; compaction, unloading, and ejection I. Design and development of a compaction calorimeter and mechanical and thermal energy determinations of powder compaction. Int. J. Pharm. 198, 113–134, 2000.

Denny P. J. Compaction equations: a comparison of the Heckel and Kawakita equations. Powder Technol. 127, 162–172, 2002.

Deveswaran R., Bharath S., Basavaraj B. V., Abraham S., Furtado S. & Madhavan V. Concepts and techniques of pharmaceutical powder mixing process: a current update. Res. J. Pharm. Tech. 2, 245–249, 2009.

DiMasi J. A., Grabowski H. G. & Hansen R. W. Innovation in the pharmaceutical industry: New estimates of R&D costs. J. Health Econ. 47, 20–33, 2016.

Doldán C., Souto C., Concheiro A., Martínez-Pacheco R. & Gómez-Amoza J.L. Dicalcium phosphate dihydrate and anhydrous dicalcium phosphate for direct compression: a comparative study. Int. J. Pharm. 124, 69–74, 1995.

Eriksson M. & Alderborn G. The effect of particle fragmentation and deformation on the interparticulate bond formation process during powder compaction. Pharm. Res. 12, 1031–1039, 1995.

Faure A., York P. & Rowe R. C. Process control and scale-up of pharmaceutical wet granulation processes: a review. Eur. J. Pharm. Biopharm. 52, 269–277, 2001.

Ferreira L. L. G. & Andricopulo A. D. ADMET modeling approaches in drug discovery. Drug Discov. Today 24, 1157–1165, 2019.

Furukawa R., Chen Y., Horiguchi A., Takagaki K., Nishi J., Konishi A., Shirakawa Y., Sugimoto M. & Narisawa S. Numerical evaluation of the capping tendency of microcrystalline cellulose tablets during a diametrical compression test. Int. J. Pharm. 493, 182–191, 2015.

Grote S. & Kleinebudde P. Roll compaction/dry granulation of dibasic calcium phosphate anhydrous–does the morphology of the raw material influence the tabletability of dry granules? J. Pharm. Sci. 107, 1104–1111, 2018.

Gupta H., Kumar S., Roy S. K. & Gaud R. S. Patent protection strategies. J. Pharm. Bioallied Sci. 2, 2–7, 2010.

Hadžović E., Betz G., Hadžidedić Š., El-Arini S. K. & Leuenberger H. Investigation of compressibility and compactibility parameters of roller compacted theophylline and its binary mixtures. Int. J. Pharm. 416, 97–103, 2011.

Hansen S. & Ottino J. M. Fragmentation with abrasion and cleavage: analytical results. Powder Technol. 93, 177–184, 1997.

Hardy I. J., Cook W. G. & Melia C. D. Compression and compaction properties of plasticised high molecular weight hydroxypropylmethylcellulose (HPMC) as a hydrophilic matrix carrier. Int. J. Pharm. 311, 26–32, 2006.

Harnby N. An engineering view of pharmaceutical powder mixing. Pharm. Sci. Tech. Today 3, 303–309, 2000.

Haware R. V., Tho I & Bauer-Brandl A. Evaluation of a rapid approximation method for the elastic recovery of tablets. Powder Technol. 202, 71–77, 2010.

Heckel R.W. Density-pressure relationships in powder compaction. Trans. Metall. Soc. AIME 221, 1001–1008, 1961.

Herting M. G. & Kleinebudde P. Roll compaction/dry granulation: Effect of raw material particle size on granule and tablet properties. Int. J. Pharm. 338, 110–118, 2007.

Herting M. G., Klose K. & Kleinebudde P. Comparison of different dry binders for roll compaction/dry granulation. Pharm. Dev. Technol. 12, 525–532, 2007.

Herting M. G. & Kleinebudde P. Studies on the reduction of tensile strength of tablets after roll compaction/dry granulation. Eur. J. Pharm. Biopharm. 70, 372–379, 2008.

Hirschberg C., Paul S., Rantanen J. & Sun C. C. A material-saving and robust approach for obtaining accurate out-of-die powder compressibility. Powder Technol. 361, 903–909, 2020.

Hu J., Johnston K. P. & Williams III R.O. Nanoparticle engineering processes for enhancing the dissolution rates of poorly water soluble drugs. Drug Dev. Ind. Pharm. 30, 233–245, 2004.

Ibrahim M., Barnes M., McMillin R., Cook D. W., Smith S., Halquist M., Wijesinghe D. & Roper T. D. 3D printing of metformin HCl PVA tablets by fused deposition modeling: drug loading, tablet design, and dissolution studies. AAPS PharmSciTech 20, 195, 2019.

Iveson S. M., Litster J. D., Hapgood K. & Ennis B. J. Nucleation, growth and breakage phenomena in agitated wet granulation processes: a review. Powder Technol. 117, 3–39, 2001.

Jain S. Mechanical properties of powders for compaction and tableting: an overview. Pharm. Sci. Technol. Today 2, 20–31, 1999.

Jennotte O., Koch N., Lechanteur A. & Evrard B. Three-dimensional printing technology as a promising tool in bioavailability enhancement of poorly water-soluble molecules: A review. Int. J. Pharm. 580, 119200, 2020.

Jivraj M., Martini L. G. & Thomson C. M. An overview of the different excipients useful for the direct compression of tablets. Pharm. Sci. Technol. Today 3, 58–63, 2000.

Juppo A. M., Kervinen L., Yliruusi J. & Kristoffersson E. Compression of lactose, glucose and mannitol granules. J. Pharm. Pharmacol. 47, 543–549, 1995.

Juppo A. M. Change in porosity parameters of lactose, glucose and mannitol granules caused by low compression force. Int. J. Pharm. 130, 149–157, 1996.

Katz J.M. & Buckner I. S. Characterization of strain rate sensitivity in pharmaceutical materials using indentation creep analysis. Int. J. Pharm. 442, 13–19, 2013.

Keizer H. L. & Kleinebudde P. Elastic recovery in roll compaction simulation. Int. J. Pharm. 573, 118810, 2020.

Keleb E. I., Vermeire A., Vervaet C. & Remon J.P. Twin screw granulation as a simple and efficient tool for continuous wet granulation. Int. J. Pharm. 273, 183–194, 2004.

Khan I., Apostolou M., Bnyan R., Houacine C., Elhissi A. & Yousaf S. S. Paclitaxel-loaded micro or nano transfersome formulation into novel tablets for pulmonary drug delivery via nebulization. Int. J. Pharm. 575, 118919, 2020.

Kipp J. E. The role of solid nanoparticle technology in the parenteral delivery of poorly water-soluble drugs. Int. J. Pharm. 284, 109–122, 2004.

Kleinebudde P. Roll compaction/dry granulation: pharmaceutical applications. Eur. J. Pharm. Biopharm. 58, 317–326, 2004.

Kolter K. & Flick D. Structure and dry binding activity of different polymers, including Kollidon® VA 64. Drug Dev. Ind. Pharm. 26, 1159–1165, 2000.

Konkel P. & Mielck J. B. Associations of parameters characterizing the time course of the tabletting process on a reciprocating and on a rotary tabletting machine for high-speed production. Eur. J. Pharm. Biopharm. 45, 137–148, 1998.

Koskela J., Morton D. A. V., Stewart P. J., Juppo A. M. & Lakio S. The effect of mechanical dry coating with magnesium stearate on flowability and compactibility of plastically deforming microcrystalline cellulose powders. Int. J. Pharm. 537, 64–72, 2018.

Kremer D. M. Anumerical investigation of air flow during tablet compression. Chem. Eng. Sci. 61, 7963–7978, 2006.

Krumme M., Schwabe L. & Frömming K.-H. Development of computerised procedures for the characterisation of the tableting properties with eccentric machines: extended Heckel analysis. Eur. J. Pharm. Biopharm. 49, 275–286, 2000.

Kuentz M. & Leuenberger H. A new theoretical approach to tablet strength of a binary mixture consisting of a well and a poorly compactable substance. Eur. J. Pharm. Biopharm. 49, 151–159, 2000.

Lamešić D., Planinšek O., Lavrič Z. & Ilić I. Spherical agglomerates of lactose with enhanced mechanical properties. Int. J. Pharm. 516, 247–257, 2017.

Late S. G. Yu Y.-Y. & Banga A. K. Effects of disintegration-promoting agent, lubricants and moisture treatment on optimized fast disintegrating tablets. Int. J. Pharm. 365, 4–11, 2009.

Leuenberger H. & Rohera B. D. Fundamentals of powder compression. I. The compactibility and compressibility of pharmaceutical powders. Pharm. Res. 3, 12–22, 1986.

Li L. C. & Peck G. E. The effect of agglomeration methods on the micromeritic properties of a maltodextrin product, Maltrin 150™. Drug Dev. Ind. Pharm. 16, 1491–1503, 1990.

Li Q., Rudolph V., Weigl B. & Earl A. Interparticle van der Waals force in powder flowability and compactibility. Int. J. Pharm. 280, 77–93, 2004.

Mangal S., Meiser F., Tan G., Gengenbach T., Morton D.A.V. & Larson I. Applying surface energy derived cohesive–adhesive balance model in predicting the mixing, flow and compaction behaviour of interactive mixtures. Eur. J. Pharm. Biopharm. 104, 110–116, 2016.

Măsić I., Ilić I., Dreu R., Ibrić S., Parojčić J. & Đurić Z. An investigation into the effect of formulation variables and process parameters on characteristics of granules obtained by in situ fluidized hot melt granulation. Int. J. Pharm. 423, 202–212, 2012.

Mazel V., Busignies V., Diarra H. & Tchoreloff P. On the links between elastic constants and effective elastic behavior of pharmaceutical compacts: importance of Poisson's ratio and use of bulk modulus. J. Pharm. Sci. 102, 4009–4014, 2013.

Michaut F., Busignies V., Fouquereau C., Huet De Barochez B., Leclerc B. & Tchoreloff P. Evaluation of a rotary tablet press simulator as a tool for the characterization of compaction properties of pharmaceutical products. J. Pharm. Sci. 99, 2874–2885, 2010.

Millán-Jiménez M., Galdón E., Ferrero C. & Caraballo I. Application of ultrasound-assisted compression in pharmaceutical technology. Design and optimization of oral sustained-release dosage forms. J. Drug. Deliv. Sci. Tech. 42, 119–125, 2017.

Mitra B., Hilden J. & Litster J. D. Novel use of monodisperse granules to deconvolute impacts of granule size versus granule solid fraction on tablet tensile strength. Adv. Powder. Technol. 26, 553–562, 2015.

Mohan S. Compression physics of pharmaceutical powders: a review. Int. J. Pharm. Sci. Res. 3, 1580–1592, 2012.

Monteyne T., Vancoillie J., Remon J.-P., Vervaet C. & De Beer T. Continuous melt granulation: Influence of process and formulation parameters upon granule and tablet properties. Eur. J. Pharm. Biopharm. 107, 249–262, 2016.

Munos B. Lessons from 60 years of pharmaceutical innovation. Nat. Rev. Drug Discov. 8, 959–968, 2009.

Muñoz-Ruiz A., Wihervaara M., Häkkinen M., Juslin M. & Paronen P. Frictional work in double-sided tablet compression. J. Pharm. Sci. 86, 481–486, 1997.

Neuhaus T. 2007. Investigation and optimisation of the Presster-a linear compaction simulator for rotary tablet presses. Doctoral dissertation, Bonn, Germany, 2007. Available online at http://hss.ulb.uni-bonn.de/2007/1152/1152.pdf—18.03.2020.

Nicklasson F., Johansson B. & Alderborn G. Occurrence of fragmentation during compression of pellets prepared from a 4 to 1 mixture of dicalcium phosphate dihydrate and microcrystalline cellulose. Eur. J. Pharm. Sci. 7, 221–229, 1999.

Nokhodchi A. An overview of the effect of moisture on compaction and compression. Pharm. Technol. 29, 46–66, 2005.

Osamura T., Takeuchi Y., Onodera R., Kitamura M., Takahashi Y., Tahara K. & Takeuchi H. Characterization of tableting properties measured with a multi-functional compaction instrument for several pharmaceutical excipients and actual tablet formulations. Int. J. Pharm. 510, 195–202, 2016.

Osei-Yeboah F., Chang S.-Y. & Sun C. C. A critical examination of the phenomenon of bonding area-bonding strength interplay in powder tableting. Pharm. Res. 33, 1126–1132, 2016.

Palmieri G. F., Joiris E., Bonacucina G., Cespi M. & Mercuri A. Differences between eccentric and rotary tablet machines in the evaluation of powder densification behaviour. Int. J. Pharm. 298, 164–175, 2005.

Passerini N., Calogerà G., Albertini B. & Rodriguez L. Melt granulation of pharmaceutical powders: A comparison of high-shear mixer and fluidised bed processes. Int. J. Pharm. 391, 177–186, 2010.

Patel S., Kaushal A. M. & Bansal A. K. Compression physics in the formulation development of tablets. Crit. Rev. Ther. Drug Carrier Syst. 23, 1–65, 2006.

Patel S., Kaushal A. M. & Bansal A. K. Effect of particle size and compression force on compaction behavior and derived mathematical parameters of compressibility. Pharm. Res. 24, 111–124, 2007.

Paul S. M., Mytelka D. S., Dunwiddie C. T., Persinger C. C., Munos B. H., Lindborg S. R. & Schacht A. L. How to improve R&D productivity: the pharmaceutical industry's grand challenge. Nat. Rev. Drug Discov. 9, 203–214, 2010.

Paul S. & Sun C. C. Gaining insight into tablet capping tendency from compaction simulation. Int. J. Pharm. 524, 111–120, 2017.

Picker K. M. Time dependence of elastic recovery for characterization of tableting materials. Pharm. Dev. Technol. 6, 61–70, 2001.

Picker K. M. The 3-D model: Comparison of parameters obtained from and by simulating different tableting machines. AAPS PharmSciTech 4, 1–7, 2003.

Pindelska E., Sokal A. & Kolodziejski W. Pharmaceutical cocrystals, salts and polymorphs: Advanced characterization techniques. Adv. Drug Deliv. Rev. 117, 111–146, 2017.

Pitt K. G. & Heasley M. G. Determination of the tensile strength of elongated tablets. Powder Technol. 238, 169–175, 2013.

Puri V., Brancazio D., Desai P. M., Jensen K. D., Chun J.-H., Myerson A. S. & Trout B. L. Development of maltodextrin-based immediate-release tablets using an integrated twin-screw hot-melt extrusion and injection-molding continuous manufacturing process. J. Pharm. Sci. 106, 3328–3336, 2017.

Razavi S. M., Gonzalez M. & Cuitiño A. M. General and mechanistic optimal relationships for tensile strength of doubly convex tablets under diametrical compression. Int. J. Pharm. 484, 29–37, 2015.

Rees J. E., Hersey J. A. & Cole E. T. Simulation device for preliminary tablet compression studies. J. Pharm. Sci. 61, 1313–1315, 1972.

Reynolds G. K., Campbell J. I. & Roberts R. J. A compressibility based model for predicting the tensile strength of directly compressed pharmaceutical powder mixtures. Int. J. Pharm. 215–224, 2017.

Roberts R. J. & Rowe R. C. The effect of punch velocity on the compaction of a variety of materials. J. Pharm. Pharmacol. 37, 377–384, 1985.

Roberts R. J. & Rowe R. C. Determination of the critical stress intensity factor (K_{IC}) of microcrystalline cellulose using radially edge-cracked tablets. Int. J. Pharm. 52, 213–219, 1989.

Rohrs B.R., Amidon G. E., Meury R. H., Secreast P. J., King H. M. & Skoug C. J. Particle size limits to meet USP content uniformity criteria for tablets and capsules. J. Pharm. Sci. 95, 1049–1059, 2006.

Rowe C. W., Katstra W. E., Palazzolo R. D. Giritlioglu B., Teung P. & Cima M. J. Multimechanism oral dosage forms fabricated by three dimensional printing. J. Control. Release 66, 11–17, 2000.

Roy J. Pharmaceutical Impurities- A Mini-Review. AAPS PharmSciTech 3, 1–8, 2002.

Ruegger C.E. & Çelick M. The effect of compression and decompression speed on the mechanical strength of compacts. Pharm. Dev. Technol. 5, 485–494, 2000.

Šantl M., Ilić I., Vrečer F. & Baumgartner S. A compressibility and compactibility study of real tableting mixtures: The impact of wet and dry granulation versus a direct tableting mixture. Int. J. Pharm. 414, 131–139, 2011.

Sarkar S., Ooi S. M., Liew C. V. & Heng P. W. S. Influence of rate of force application during compression on tablet capping. J. Pharm. Sci. 104, 1319–1327, 2015.

Seem T. C., Rowson N. A., Ingram A., Huang Z., Yu S., De Matas M., Gabbott I. & Reynolds G. K. Twin screw granulation — A literature review. Powder Technol. 276, 89–102, 2015.

Shang C., Sinka I. C., Jayaraman B. & Pan J. Break force and tensile strength relationships for curved faced tablets subject to diametrical compression. Int. J. Pharm. 442, 57–64, 2013.

Shekunov B. Y., Chattopadhyay P., Tong H. H. Y. & Chow A. H. L. Particle size analysis in pharmaceutics: principles, methods and applications. Pharm. Res. 24, 203–227, 2007.

Shi L. & Sun C. C. Overcoming Poor Tabletability of Pharmaceutical Crystals by Surface Modification. Pharm. Res. 28, 3248–3255, 2011.

Shi L., Feng Y. & Sun C. C. Massing in high shear wet granulation can simultaneously improve powder flow and deteriorate powder compaction: A double-edged sword. Eur. J. Pharm. Sci. 43, 50–56, 2011.

Singhal D. & Curatolo W. Drug polymorphism and dosage form design: a practical perspective. Adv. Drug Deliv. Rev. 56, 335–347, 2004.

Sinka I. C., Motazedian F., Cocks A. C. F. & Pitt K. G. The effect of processing parameters on pharmaceutical tablet properties. Powder Technol. 189, 276–284, 2009.

Snider D. A., Addicks W. & Owens W. Polymorphism in generic drug product development. Adv. Drug Deliv. Rev. 56, 391–395, 2004.

Sonnergaard J. M. A critical evaluation of the Heckel equation. Int. J. Pharm. 193, 63–71, 1999.

Sonnergaard J. M. Quantification of the compactibility of pharmaceutical powders. Eur. J. Pharm. Biopharm. 63, 270–277, 2006.

Stahly P. G. Diversity in single- and multiple-component crystals. The search for and prevalence of polymorphs and cocrystals. Cryst. Growth Des. 7, 1007–1026, 2007.

Suihko E., Lehto V.-P., Ketolainen J., Laine E. & Paronen P. Dynamic solid-state and tableting properties of four theophylline forms. Int. J. Pharm. 217, 225–236, 2001.

Sun C. C. Setting the bar for powder flow properties in successful high speed tableting. Powder Technol. 201, 106–108, 2010.

Sun C. C. Decoding powder tabletability: roles of particle adhesion and plasticity. J. Adhes. Sci. Technol. 25, 483–499, 2011.

Sun C. & Grant D. J. W. Effects of initial particle size on the tableting properties of L-lysine monohydrochloride dihydrate powder. Int. J. Pharm. 215, 221–228, 2001 (a).

Sun C. & Grant D. J. W. Influence of elastic deformation of particles on heckel analysis. Pharm. Dev. Technol. 6, 193–200, 2001 (b).

Sun C. C. & Himmelspach M. W. Reduced tabletability of roller compacted granules as a result of granule size enlargement. J. Pharm. Sci. 95, 200–206, 2006.

Sun C. C. & Kleinebudde P. Mini review: Mechanisms to the loss of tabletability by dry granulation. Eur. J. Pharm. Biopharm. 106, 9–14, 2016.

Suresh P., Sreedhar I., Vaidhiswaran R. & Venugopal A. A comprehensive review on process and engineering aspects of pharmaceutical wet granulation. Chem. Eng. J. 328, 785–815, 2017.

Tan M. X. L., Nguyen T. H. & Hapgood K. P. Drug distribution in wet granulation: foam versus spray. Drug Dev. Ind. Pharm. 39, 1389–1400, 2013.

Thompson M. R., Weatherley S., Pukadyil R. N. & Sheskey P. J. Foam granulation: new developments in pharmaceutical solid oral dosage forms using twin screw extrusion machinery. Drug Dev. Ind. Pharm. 38, 771–784, 2012.

Thoorens G., Krier F., Leclercq B., Carlin B. & Evrard B. Microcrystalline cellulose, a direct compression binder in a quality by design environment—A review. Int. J. Pharm. 473, 64–72, 2014.

Tye C. K., Sun C. C. & Amidon G. E. Evaluation of the effects of tableting speed on the relationships between compaction pressure, tablet tensile strength, and tablet solid fraction. J. Pharm. Sci. 94, 465–472, 2005.

Van Den Ban S. & Goodwin D. J. The impact of granule density on tabletting and pharmaceutical product performance. Pharm. Res. 34, 1002–1011, 2017.

Van Der Voort Maarschalk K., Zuurman K., Vromans H., Bolhuis G. K. & Lerk C. F. Porosity expansion of tablets as a result of bonding and deformation of particulate solids. Int. J. Pharm. 140, 185–193, 1996.

Van Der Voort Maarschalk K., Zuurman K., Vromans H., Bolhuis G. K. & Lerk C. F. Stress relaxation of compacts produced from viscoelastic materials. Int. J. Pharm. 151, 27–34, 1997.

Venables H. J. & Wells J. I. Powder mixing. Drug Dev. Ind. Pharm. 27, 599–612, 2001.

Vercruysse J., Díaz D. C., Peeters E., Fonteyne M., Delaet U., Van Assche I., De Beer T., Remon J. P. & Vervaet C. Continuous twin screw granulation: Influence of process variables on granule and tablet quality. Eur. J. Pharm. Biopharm. 82, 205–211, 2012.

Walker G. M., Andrews G. & Jones D. Effect of process parameters on the melt granulation of pharmaceutical powders. Powder Technol. 165, 161–166, 2006.

Worku Z. A., Kumar D., Gomes J. V., He Y., Glennon B., Ramisetty K. A., Rasmuson Å. C., O'Connell P., Gallagher K. H. Woods T., Shastri N. R. & Healy A.-M. Modelling and understanding powder flow properties and compactability of selected active pharmaceutical ingredients, excipients and physical mixtures from critical material properties. Int. J. Pharm. 531, 191–204, 2017.

Wu C.-Y. DEM simulations of die filling during pharmaceutical tabletting. Particuology 6, 412–418, 2008.

Wu C.-Y., Hancock B. C., Mills A., Bentham A. C., Best S. M. & Elliott J. A. Numerical and experimental investigation of capping mechanisms during pharmaceutical tablet compaction. Powder Technol. 181, 121–129, 2008.

Wurster D. E., Rowlings C. E. & Creekmore J. R. Calorimetric analysis of powder compression: I. Design and development of a compression calorimeter. Int. J. Pharm. 116, 179–189, 1995.

Zavaliangos A., Katz J. M., Daurio D., Johnson M., Pirjanian A. & Alvarez-Nunez F. Prediction of air entrapment in tableting: an approximate solution. J. Pharm. Sci. 106, 3604–3612, 2017.

Zhang J., Wu L., Chan H.-K. & Watanabe W. Formation, characterization, and fate of inhaled drug nanoparticles. Adv. Drug Deliv. Rev. 63, 441–455, 2011.

Zhang C., Xiong Y., Jiao F., Wang M. & Li H. Redefining the term of "cocrystal" and broadening its intention. Cryst. Growth Des. 19, 1471–1478, 2019.

Zhu T., Li J. & Yip S. Atomistic study of dislocation loop emission from a crack tip. Phys. Rev. Lett. 93, 025503, 2004.

Zhu X.-K. & Joyce J. A. Review of fracture toughness (G, K, J, CTOD, CTOA) testing and standardization. Eng. Fract. Mech. 85, 1–46, 2012.

Supplementary information

MATLAB-code with exemplary values entered:

```
clc
clear all
%%% G-HVC DATA ANALYSIS PROGRAM V 1.1 BY OSMO ANTIKAINEN
%%% (EDITED BY TIMO TANNER)
[fileName,PathName] = uigetfile2('*.csv');
%%%(uigetfile2 is a separate program for retrieving the file)
Nimi=fullfile(PathName,fileName);
%(fullfile is a separate program combining path name and file name)
%CHOOSE RADIUS, WEIGHT AND TRUE DENSITY
r=4.1/1000;
mass=0.0138;
%%%Radius (r) in metres so that pressure calculus works
%%%% mass (weight) in grams and dimension in centimetres so that g/cm3
%CHOOSE CSV OR XLS FILE
%(csvread and xlsread are separate programs reading these files)
M = csvread(Nimi,0,2);
v=size(M);v=v(1);
k=0;
for i= 1:v
   if M(i,1)>-20;
      k=k+1;
      y1(k)=-M(i,1)/1000;
      y2(k)=M(i,2)/1000;
      t(k)=(1/20000)*k;
   end
end
%M1=xlsread(Nimi,'A:A');
%M2=xlsread(Nimi,'B:B');
%v=size(M1);v=v(1);
%for i=1:v
   %if M1(i)>-20;
      %k=k+1;
      %y1(k)=-M1(i)/1000;
      %y2(k)=-M2(i)/1000;
      %t(k)=(1/20000)*k;
   %end
%end
%%%Pharmatose 80M
%TrueD=1.523
%%%Pharmatose 200M
```

```
%TrueD=1.515
%%%Vivapur 101
%TrueD=1.522
%%%Avicel PH-102
%TrueD=1.519
%%%Avicel PH-200
%TrueD=1.535
%%%Glucose, anhydr.
%TrueD=1.556
%%%Calcium hydrogen phosphate
%TrueD=2.624
%%%Starch 1500
%TrueD=1.477
%Enter value freely
TrueD=1.5;
t=t';
y1=y1';
MaxDispBar=min(y1);
A=k(end);
M_FinalDispBar=y1(A);
[xmin,i]=min(y1); %xmin, pohja (bar)
for d=1:i+2000
   Den(d)=mass/(100*r*100*r*3.1415926*y1(d)*100);
   Porosity(d)=100-((Den(d)/TrueD)*100);
end
for j=1:i+2000
y11(j)=y1(j)-y1(1);
y1d(j)=y1(j);
y21(j)=y2(j)-y2(1);
t2(j)=t(j);
end
y11sg=sgolayfilt(y11,2,21);
y21sg=sgolayfilt(y21,2,21);
y1dsg=sgolayfilt(y1d,2,7);
%Speed from filtered (bar and base)
%sgolayfilt is a separate program executing Savitzky-Golay filtering
%sigm_fit is a separate program executing sigmoidal fit
for ii=1:i+1999
   V(ii)=(y11sg(ii+1)-y11sg(ii))/(t2(ii+1)-t2(ii));
   %V(ii)=(y11(ii+1)-y11(ii))/(t2(ii+1)-t2(ii));
   Vbase(ii)=(y21sg(ii+1)-y21sg(ii))/(t2(ii+1)-t2(ii));
   Vbaseun(ii)=(y21(ii+1)-y21(ii))/(t2(ii+1)-t2(ii));
   t3(ii)=(t2(ii+1)+t2(ii))/2;
end
```

```
V_sg=sgolayfilt(V,1,11);
MaxVeloBar=(-1)*min(V);
MinVeloBase=min(Vbase);
MinVelobasePlus=(-1)*MinVeloBase;
MaxDispBarZero=(-1)*min(y11);
%Acceleration
for iii=1:i+1998
   a(iii)=(V(iii+1)-V(iii))/(t3(iii+1)-t3(iii));
   a1(iii)=(V_sg(iii+1)-V_sg(iii))/(t3(iii+1)-t3(iii));
   t4(iii)=(t3(iii+1)+t3(iii))/2;
end
a_sg=sgolayfilt(a1,2,11);
a_sg_fall=sgolayfilt(a1,2,301);
F=(a_sg+9.48)*6.35;
unF=(a+9.48)*6.35;
j=i;
while F(j)>0
   j=j-1;
   tstart=t4(j);
   xstart=y1(j);
end
j2=i;
while F(j2)>0
   j2=j2+1;
   tend=t4(j2);
   xend=y1(j2);
end
V_cut=V(j-10:j2+15);
t_cut=t2(j-10:j2+15);
y1_cut=y1(j-10:j2+15);
Porosity_cut=Porosity(j:j2);
y1_contact=y1(j:j2);
y1_contact_mm=y1_contact*1000;
V_contact=V(j:j2);
t_contact=t2(j:j2);
x=t_cut;
y=V_cut;
figure(1)
[param,stat]=sigm_fit(x,y);
SigmV=stat.ypred;
SigmV=SigmV';
%figure(2)
%plot(t_contact,y1_contact_mm);
%figure(2)
```

```
%plot(t_cut,SigmV);
%figure(2)
%plot(t_contact,V_contact);
M_t_contact=tend-tstart;
MB_contact_ms=M_t_contact*1000;
%figure(3)
%plot(t_contact,y1_contact);
%figure(3)
%plot(t_cut,y1_cut);
%%%xlswrite('testdata.xlsx',t_cut')
%%%xlswrite('testdata.xlsx',y1_cut,1,'B1') USE THIS FOR EXCEL
CutSize=size(V_cut);
for j=1:CutSize(2)-1
a_cut(j)=(SigmV(j+1)-SigmV(j))/(t_cut(j+1)-t_cut(j));
ta(j)=(t_cut(j+1)+t_cut(j))/2;
end
a_cut_sg=sgolayfilt(a_cut,2,21);
F_cut=(a_cut+9.48)*6.35;
P_cut=F_cut/(r*r*3.14159265);
P_cut_MPa=P_cut/1000000;
MaxForce=max(F_cut);
MaxPressure=max(P_cut)/1000000;
%MaxPressure in MPa
MaxDensity=mass/(r*100*r*100*3.14159265*MaxDispBar*100);
M_FinalDensity=mass/(r*100*r*100*3.14159265*M_FinalDispBar*100);
%{
figure(3)
plot(ta,a_cut);
figure(4)
plot(ta,F_cut);
figure(5)
plot(ta,P_cut_MPa);
%}
%{
td_Porosity_cutExcel=Porosity_cut';
t_contact_ms=t_contact*1000;
tContact_Excel=t_contact_ms';
tContact_y1_Excel=y1_contact;
tC_SpringbackVmax=max(V_contact);
%}
figure(2);
plot(t3,Vbase);
%figure(3);
%plot(t,y1);
```